U.PORTO

MESTRADO EM ONCOLOGIA

ESPECIALIZAÇÃO EM ONCOLOGIA MOLECULAR

Study of the antitumor potential of natural products and curcumin-loaded PLGA nanoparticles in human breast cancer cell lines

Daniela Filipa Rodrigues Figueiredo

M

2018

U.PORTO

Daniela Filipa Figueiredo. Study of the antitumor potential of natural products and curcumin-loaded PLGA nanoparticles in human breast cancer cell lines

M.ICBAS 2018

Study of the antitumor potential of natural products and curcumin-loaded PLGA nanoparticles in human breast cancer cell lines

Daniela Filipa Rodrigues Figueiredo

INSTITUTO DE CIÊNCIAS BIOMÉDICAS ABEL SALAZAR

Daniela Filipa Rodrigues Figueiredo

Study of the antitumor potential of natural products and curcumin-loaded PLGA nanoparticles in human breast cancer cell lines

Dissertação de Candidatura ao grau de Mestre em Oncologia – Especialização em Oncologia Molecular, submetida ao Instituto de Ciências Biomédicas Abel Salazar da Universidade do Porto.

Orientador – Prof. Doutora M. Helena Vasconcelos
Categoria – Professor Auxiliar
Afiliação – Departamento de Ciências Biológicas da Faculdade de Farmácia da Universidade do Porto e Coordenadora do Grupo Cancer Drug Resistance do Instituto de Patologia e Imunologia Molecular da Universidade do Porto/Instituto de Investigação e Inovação em Saúde da Universidade do Porto

Coorientador – Tamara Fernández Marcelo
Categoria – Investigadora
Afiliação – Grupo Cancer Drug Resistance do Instituto de Patologia e Imunologia Molecular da Universidade do Porto/Instituto de Investigação e Inovação em Saúde da Universidade do Porto

Coorientador- Carmen Jerónimo
Categoria – Professor Associado Convidado
Afiliação – Instituto de Ciências Biomédicas Abel Salazar da Universidade do Porto
Investigadora Auxiliar e Coordenadora do Grupo de Epigenética e Biologia do Cancro - Centro de Investigação do Instituto Português de Oncologia do Porto Francisco Gentil, E.P.E.

INFORMAÇÃO TÉCNICA

TÍTULO:
Study of the antitumor potential of natural products and curcumin-loaded PLGA nanoparticles in human breast cancer cell lines

Dissertação de candidatura ao grau de Mestre em Oncologia – especialização em Oncologia Molecular, apresentada ao Instituto de Ciências Biomédicas de Abel Salazar da Universidade do Porto

AUTOR:
Daniela Filipa Rodrigues Figueiredo

DATA:
Outubro de 2018

EDITOR: Daniela Filipa Rodrigues Figueiredo
CORREIO ELETRÓNICO: danielafilipa.1995@hotmail.com
1ª EDIÇÃO: Outubro de 2018

“Somewhere, something incredible is waiting to be known.”

Carl Sagan

Acknowledgements

Chegada ao fim esta importante etapa da minha vida, não poderia deixar de agradecer aos que, que de uma forma ou de outra, também contribuíram para a realização deste projeto.

Em primeiro lugar, gostaria de agradecer à minha orientadora, a Prof. Doutora Maria Helena Vasconcelos, por me ter aceite na sua equipa e ter tornado possível a realização deste projeto. Obrigada por todo o conhecimento que me transmitiu, pelas palavras sábias, pelo apoio e motivação.

À Prof. Doutora Carmen Jerónimo por me ter concedido a oportunidade de ingressar neste ciclo de estudos e pela sua coorientação neste trabalho.

À Doutora Tamara Fernández Marcelo, mais do que minha coorientadora, uma amiga. Obrigada pelo teu companheirismo, pelo teu sentido crítico, por estares sempre presente, pela paciência e pelo suporte. Estou muito grata por te ter conhecido e ter passado este ano contigo, ensinaste-me muito do que sei hoje e por isso te devo um agradecimento muito especial. Quero agradecer-te por todos os bons momentos, por todas as horas que passámos fechadas na sala de cultura, pelas longas batalhas de citometria fora de horas onde tudo nos acontecia. Obrigada por toda a confiança, pela tua boa disposição e amizade! Sem ti dificilmente este trabalho teria sido concretizado!

À Prof. Isabel Ferreira, do Centro de Investigação de Montanha (CIMO), Instituto Politécnico de Bragança, pela preparação dos extratos de plantas testados neste trabalho.

A todo o grupo Cancer Drug Resistance, pela amizade, entreajuda e partilha. Por terem sempre uma palavra amiga e por tentarem sempre ajudar qualquer que seja a situação.

Ao Doutor Tiago dos Santos, do INEB/i3S, por todo o conhecimento que me transmitiu sobre nanopartículas. Um obrigado por estares sempre disponível e por me teres acompanhado sempre que precisei.

A todos os colegas e amigos que conheci no i3s, obrigada pelos momentos de descontração, pela amizade e simpatia! Obrigada por todo o apoio que me deram, por dizerem sempre uma palavra amiga nos momentos em que as coisas corriam menos bem e por saber que podia sempre contar convosco.

À Rita, mais do que uma colega de curso e de casa, uma amiga para a vida! Foste tu quem me fez dar o primeiro passo, quem me motivou e não me deixou desistir. Obrigada

por estares sempre presente, por me ouvires, por todos os teus conselhos e ajuda. Aprendi muito contigo e sem ti não teria sido a mesma coisa! Passámos muito tempo juntas, momentos tristes, momentos alegres, momentos de desespero (principalmente nestes últimos meses) e chegámos juntas até ao fim! Quero que saibas que podes sempre contar comigo para tudo, assim como pude contar contigo!

Ao Micael, por ter sido o meu maior apoio nesta longa jornada. Obrigada por estares sempre disponível quando mais preciso, por seres atencioso, meigo e por conseguires sempre fazer-me sentir melhor, qualquer que seja a situação. Obrigada por seres compreensivo em todos os meus momentos de mau-humor. Por acreditares sempre em mim e nunca me deixares desistir. Obrigada por tudo o que fazes por mim!

Ao meu irmão, Diogo, por me testar a paciência ao limite! A verdade é que estas coisas fazem parte e no fundo eu sei que gostas tanto de mim como eu de ti. Obrigada por toda a ajuda que me dás, por me apoiares (às vezes!) e por me acompanhares sempre. Espero que saibas que tenho muito orgulho em ti!

Aos meus avós e à minha tia por acreditarem em mim, por me terem acompanhado sempre ao logo do meu percurso, sempre com orgulho. Por vocês sinto uma grande admiração e respeito. Obrigada por tudo o que fazem por mim!

Por fim finalizo os meus agradecimentos com um profundo obrigado aos meus pais, sem eles nada disto seria possível! Obrigada por me apoiarem sempre, por acreditarem em mim, por me ajudarem sempre e por estarem sempre do meu lado. É graças a vocês que cheguei até aqui! Obrigada por terem orgulho em mim e por todo o esforço que fazem para nos darem um futuro melhor! Vocês são o meu orgulho!

Abstract

Breast cancer (BC) is the second most common cancer worldwide and the most frequent cancer among women, in developed and underdevelopment nations. In Portuguese women, BC is the most prevalent malignancy, with an incidence of 67.6 cases per 100 000 people. BC is a complex and heterogeneous disease composed by a growing number of molecular subtypes, which affects the therapeutic response and disease progression. Triple negative breast cancer (TNBC) represents 15-20% of all breast cancers and is the most heterogeneous group from all the subtypes, presenting an aggressive phenotype, high histologic grade and high levels of proliferation and invasion, with an extremely poor prognosis and shortest survival.

Accumulating evidence suggests that tumor initiation and proliferation abilities rely on a small population of stem-like cells, named as cancer stem cells (CSC). CSCs are believed to be responsible for resistance to conventional cancer therapies and treatment failure. Therefore, the isolation, characterization and targeting of CSCs has significant therapeutic implications in cancer research.

Natural products have gained important attention in cancer treatment due to their availability and since they are a source of bioactive compounds, many of them having antitumor potential. Indeed, some natural products are capable of inhibiting tumor cell proliferation pathways without affecting the non-tumor cells. In particular, curcumin (CUR) is a natural product and a promising compound with antitumor activity. However, CUR has poor bioavailability and therefore different approaches have been attempted (including curcumin-loaded nanoparticles) to improve its efficacy.

Therefore, the main aims of this work were to: i) analyze the antitumor activity of natural extracts/compounds (*Melissa Officinalis L., Eucalyptus globulus L*. and Curcumin) in human breast cancer cell lines; ii) develop Curcumin loaded poly(lactic-co-glycolic acid), PLGA, nanoparticles; iii) analyze the antitumor activity of the Curcumin loaded PLGA nanoparticles in human breast cancer cell lines; iv) characterize and isolate breast cancer stem cells (CSCs) from the Hs 578T cell line; and v) evaluate the cytotoxic effect of CUR and Curcumin loaded PLGA nanoparticles in sorted stem cells from the Hs 578T breast cancer cell line.

To address these objectives, two breast cell lines were used: the BT-20 cell line and the Hs 578T cell line, both representative of TNBC. The antitumor activity of the natural extracts *Eucalyptus globulus L.* and *Melissa officinalis L.* was tested in both cell lines with the Sulforhodamine B (SRB) assay, following 48-hour treatments. Results showed that these extracts were more potent in the Hs 578T cell line than in the BT-20 cell line, and that all the extracts exhibit similar inhibitory effect in each of the cell lines.

In an attempt to improve CUR bioavailability and solubility, a Curcumin loaded PLGA nanoparticle was developed via a nanoprecipitation technique. Three different initial concentrations of CUR were tested (0.1mg, 0.5 mg and 1 mg). The CUR-loaded nanoparticles prepared with an initial CUR concentration of 0.5 mg were selected for the *in vitro* cytotoxic experiments, since they presented a smaller particle size ($241 \pm 9.2_{nm}$), a higher percentage of encapsulation (63 ± 3%) and an homogeneous formulation (PDI = 0,1 ± 0,01). Following the calculation of the GI_{50} concentration for these CUR-loaded nanoparticles, when compared with CUR alone, it was concluded that the CUR-loaded nanoparticles caused less tumor cell growth inhibition than free CUR.

The characterization and isolation of Hs 578T stem-like cells ($ALDH^+/CD44^{high}$) and non-stem like cells ($ALDH^-/CD44^{low}$) was performed using the ALDEFLUOR™ kit in combination with allophycocyanin (APC)-conjugated anti-CD44. Preliminary flow cytometric analysis revealed that the Hs 578T cell line is enriched in $CD44^+$ cells and the $ALDH^+$ population was detected in the 21.1% of the Hs 578T cells. Therefore, attempts to isolate the CSCs and non-stem cells were made. However, although it was possible to isolate some stem-like cells, not enough number of CSCs were obtained to allow to test the CUR and CUR-loaded nanoparticles.

In summary, the obtained results indicate that both natural extracts tested, and the CUR and CUR nanoparticles, have dose-dependent tumor cell growth inhibitory effects in the cell lines tested. However, there was no evidence that the CUR-loaded nanoparticles had a more potent effect than free CUR, when the cytotoxic effects were compared following the same treatment time points.

In addition, preliminary results suggest that it is possible to isolate stem-like cells from the Hs 578T cell line. However, this needs further optimization in order to obtain more CSCs to allow the study of the effect of CUR and CUR nanoparticles, or other compounds and extracts, in the selected sorted stem cells from this cell line.

Keywords: Cancer; antitumor activity; natural products; *Melissa Officinalis L.; Eucalyptus globulus L,*; Curcumin; Curcumin loaded PLGA nanoparticles; CSC; ALDH1; CD44

Resumo

O cancro de mama é o segundo tipo de cancro mais frequente no mundo e o mais frequente entre as mulheres, tanto em países desenvolvidos como em desenvolvimento. Nas mulheres portuguesas, o cancro de mama é a neoplasia maligna mais prevalente, com uma incidência de 67,6 casos por 100 000 pessoas. O cancro de mama é uma doença complexa e heterogénea, composta por um número crescente de subtipos moleculares, o que afeta a resposta terapêutica e a progressão da doença. O cancro de mama triplo negativo (TNBC) representa 15-20% de todos os cancros de mama, é o grupo mais heterogéneo de todos os subtipos, apresentando um fenótipo agressivo, alto grau histológico e altos níveis de proliferação e invasão, com um mau prognóstico e baixa sobrevivência.

Várias evidências sugerem que a iniciação e proliferação tumoral dependem de uma pequena população de células semelhantes a células estaminais *("stem-like")*, designadas por células estaminais cancerígenas (CSC). Pensa-se que as CSCs são as responsáveis pela resistência às terapias antineoplásicas convencionais e à falha do tratamento. Portanto, o isolamento e caracterização destas células, assim como o desenvolvimento de terapias dirigidas às CSCs, têm implicações terapêuticas significativas na investigação oncológica.

Os produtos naturais têm recebido importante atenção no tratamento do cancro devido à sua disponibilidade e uma vez que são uma fonte de compostos bioativos, muitos deles tendo atividade antitumoral. De facto, alguns produtos naturais têm a capacidade de inibir vias de proliferação de células tumorais sem afetar as células não tumorais. Em particular, a curcumina (CUR) é um produto natural e é considerada um promissor composto com atividade antitumoral. No entanto, a CUR tem uma baixa biodisponibilidade e, portanto, diferentes abordagens têm sido testadas (incluindo nanopartículas contendo curcumina) de forma a melhorar a sua eficácia.

Assim sendo, os principais objetivos do presente trabalho foram: i) analisar a atividade antitumoral de extratos naturais/compostos (*Melissa Officinalis L., Eucalyptus globulus L*. e curcumina) em linhas celulares de cancro de mama; ii) desenvolver nanopartículas de poli(ácido láctico-co-glicólico), PLGA, contendo curcumina; iii) analisar a atividade antitumoral das nanopartículas de PLGA carregadas com curcumina em linhas celulares de cancro de mama; iv) caracterizar e isolar, a partir da linha celular Hs 578T, células estaminais de cancro de mama (CSCs) e v) avaliar o efeito citotóxico da CUR e das

nanopartículas de PLGA carregadas com curcumina em células estaminais isoladas da linha celular de cancro de mama Hs 578T.

Para alcançar estes objetivos, duas linhas celulares de cancro de mama foram usadas: a linha celular BT-20 e a linha celular Hs 578T, ambas representativas do TNBC. A atividade antitumoral dos extratos naturais *Eucalyptus globulus L.* e *Melissa officinalis L.* foi testada nas duas linhas celulares através do ensaio de Sulforrodamina B (SRB), após 48h de tratamento. Os resultados mostraram que estes extratos foram mais potentes na linha celular *Hs 578T* do que na linha celular BT-20, e que todos os extratos exibiram um efeito inibitório semelhante em cada linha celular.

Numa tentativa de melhorar a biodisponibilidade e solubilidade da CUR, foram desenvolvidas nanopartículas de PLGA carregadas com curcumina através da técnica de nano-precipitação. Três diferentes concentrações iniciais de curcumina foram testadas (0,1 mg; 0,5 mg e 1 mg). As nanopartículas de curcumina preparadas com uma concentração inicial de 0,5 mg de CUR foram selecionadas para os ensaios de citotoxicidade *in vitro,* por apresentarem um menor tamanho de partículas (241 ± 9,2nm), uma maior percentagem de encapsulação (63 ± 3%) e uma formulação homogénea (PDI = 0,1 ± 0,01). Após o cálculo da concentração do valor de GI_{50} para estas nanopartículas de PLGA carregadas com curcumina, concluiu-se que, quando comparadas com a CUR livre, as nanopartículas de curcumina causaram uma menor inibição do crescimento das células tumorais do que o tratamento com curcumina livre.

A caracterização e isolamento de células estaminais ($ALDH^+/CD44^{high}$) e não estaminais ($ALDH^-/CD44^{low}$), a partir da linha celular Hs 578T, foi realizada utilizando o kit ALDEFLUOR™ em combinação com anticorpo anti-CD44 conjugado com allophycocyanin (APC). Análises preliminares por citometria de fluxo revelaram que a linha celular Hs 578T é enriquecida em células $CD44^+$ e que a população $ALDH^+$ foi detetada em 21,1% das células Hs 578T. Por conseguinte, foram feitas tentativas para isolar CSCs e células *non-stem*. No entanto, embora tenha sido possível isolar algumas células *stem-like*, não foi obtido o número de CSCs necessário para testar a CUR e nanopartículas carregadas com curcumina.

Em resumo, os resultados obtidos indicam que ambos os extratos naturais testados, assim como a curcumina e as nanopartículas de curcumina, possuem efeitos inibidores do crescimento dependentes da dose, nas células tumorais testadas. No entanto, não houve evidencia de que as nanopartículas carregadas com curcumina tenham um efeito mais potente do que a CUR livre, quando os efeitos citotóxicos foram testados após os mesmos tempos de tratamento.

Adicionalmente, resultados preliminares sugerem que é possível isolar células *stem-like* da linha celular Hs 578T. No entanto, são necessárias mais otimizações de forma a se

obterem mais CSCs, de forma a permitir o estudo do efeito da CUR e de nanopartículas de curcumina, ou de outros compostos e extratos, em CSCs isoladas a partir desta linha celular.

Palavras Chave: Cancro; atividade antitumoral; produtos naturais; *Melissa Officinalis L.; Eucalyptus globulus L.; curcumina; nanopartículas de PLGA carregadas com curcumina; CSC; ALDH1; CD44*

Table of contents

Index of Figures

Index of Tables

List of abbreviations

7-AAD	7-Actinoaminomycin-D
ABC	ATP - Binding Cassette
ALDH1	Aldehyde Dehydrogenase 1
APC	Allophycocyanin
ASW	Age-standardized rate
BAA	BODIPY-Aminoacetate
BAAA	BODIPY-Aminoacetaldehyde
BC	Breast Cancer
BL1	Basal-like 1
BL2	Basal-like 2
CDKs	Cyclin-Dependent Kinases
CIMO	Mountain Research Center
CSC	Cancer Stem Cells
CUR	Curcumin
DEAB	Diethylaminobenzaldehyde
DI	Deionized
DLS	Dynamic Light Scatering
DMSO	Dimethyl Sulfoxide
EE	Encapsulation Efficiency
EGFR	Epidermal Growth Factor Receptor
EMT	Epithelial-to-Mesenchymal Transition
ER	Estrogen Receptor
FBS	Fetal Bovine Serum
FITC	Fluorescein isothiocyanate
FSC	Forward scatter channel
GI_{50}	Concentration that cause 50% inhibition of cell growth
HA	Hyaluronic Acid
HER-2	Human Epidermal Growth Factor Receptor
IC_{50}	Inhibitory concentration of 50%
IM	Immunomodulatory
LAR	Luminal androgen receptor
M	Mesenchymal
MME	Membrane metalloendopeptidase

MMPs	Matrix Metalloproteinases
MSL	Mesenchymal stem-like
MW	Molecular weight
NF-κB	Nuclear factor kappa B
NPs	Nanoparticles
OD	Optical density
O/N	Over night
PDI	Polydispersity Index
PEG	Polyethylene glycol
PGA	Polyglycolic Acid
P-gp	P-glycoprotein
PLA	Polylactic Acid
PLGA	Poly (lactic-co-glycolic acid)
PMT	Photomultiplier Tube
PR	Progesterone Receptor
Ptch1	Patched 1
PVA	Poly(vinyl alcohol)
RhoA	Ras homolog gene family, member A
ROS	Reactive oxygen species
RT	Room temperature
SRB	Sulforhodamine B
SSC	Side scatter channel
STAT3	Signal Transducer and Activator of Transcription 3
TCA	Trichloroacetic Acid
TNBC	Triple Negative Breast Cancer
VEGF	Vascular Endothelial Growth Factor

Introduction

1. Cancer: An overview

Cancer development is a growing health problem. It represents the leading cause of death worldwide, with >14 million new cases and 8.2 million cancer deaths estimated to have occurred in 2012. These numbers are expected to increase in the following years, largely due to the growth and aging of population and lifestyle habits [2-4].

Cancer remains a complex and heterogeneous disease involving numerous changes in cell genetics, epigenetics and physiology, leading to abnormal cell capabilities such as cell growth, immortality, escape from apoptosis, invasion and metastasis, among others. Several efforts have been made to understand how normal cells are transformed into malignant cells and the origin of this disease [5].

Nowadays it is known that carcinogenesis is a multistep and complex process that involves the accumulation of genetic and epigenetic alterations and affects cellular pathways and processes e.g. differentiation, proliferation, invasion and survival [6-8].

The mutations that promote carcinogenesis generally occur mainly in two types of genes: proto-oncogenes and tumor-suppressor genes. Proto-oncogenes encode proteins involved in cell growth and proliferation and, when mutated, a proto-oncogene is called an oncogene. An oncogene can be constitutively active or active under special conditions that do not happen in a healthy cell, leading to an abnormal cell proliferation. Tumor suppressor genes act to inhibit cell proliferation, and when mutated, their function is lost, leading to a continuous proliferation of tumor cells. Mutations in these genes can occur in the germline or in single somatic cells. Germline mutations result in hereditary predisposition to cancer and people with these mutations develop tumors at an earlier age. The somatic mutations result in sporadic tumors, in which the first somatic mutation initiates the neoplastic process and subsequent somatic mutations result in tumor progression [9, 10]. In some cases, this knowledge allows to develop a personalized and more effective therapy.

Even so, genetic data mainly gives us information about the increased risk to develop the disease, nonetheless, the lifestyle habits and the interactions with environmental factors have a pivotal role in cancer development [11].

The lifestyle habits that are a risk factor for cancer include smoking, alcohol consumption, obesity and sedentarism. Smoking is well known as a major risk factor for cancer development, accounting for 25-30% of all deaths from cancer, mainly due to the mutagenic compounds present in tobacco. Chronic alcohol consumption is a risk factor for cancers of the upper aerodigestive tract (oral cavity, larynx, pharynx and esophagus), pancreas, liver and breast. It is known that alcohol *per se* is not mutagenic, acting mainly as a

cocarcinogen; however, it is not fully understood how it contributes to carcinogenesis. Being overweight or obese also increases the risk of cancer.

Other environmental factors include some infectious agents, radiation and pollutants. About 17.8% of tumors are associated with infections worldwide, being viruses the most prevalent infectious agents. Cancers induced by radiation account for 10% of all cancers and these include cases of exposure to ionizing and non-ionizing radiation, mostly from ultraviolet, pulsed electromagnetic fields and radioactive substances. Exposure to some pollutants was also associated with the risk for development of some cancers. Such pollutants comprise carbon particles, volatile organic compounds and tobacco smoke, food additives usage and by carcinogenic contaminants, some medicines and carcinogenic metals [11, 12].

1.1. The hallmarks of cancer

Cancer genes, and their molecular contribution to cancer have been summarized and categorized to rationalize and organize the complexity of the disease [13]. Cancer features were termed as the “hallmarks of cancer”. These hallmarks were first described, in the year 2000, by Doctors Hanahan and Weinberg [6]. They initially summarized the dense complexities of the neoplastic disease into six major hallmarks: insensitivity to antigrowth signals, evasion from programmed cell death, self-sufficiency in growth signals, tissue invasion and metastasis, sustained angiogenesis, and limitless replicative potential [6]. A decade later, they updated their summary of the hallmarks of cancer, to incorporate two emerging hallmarks (**Figure 1**): evasion from the immune response and alterations in energy metabolism. In addition, they suggested two enabling traits: genome instability and mutation, and tumor-promoting inflammation [10].

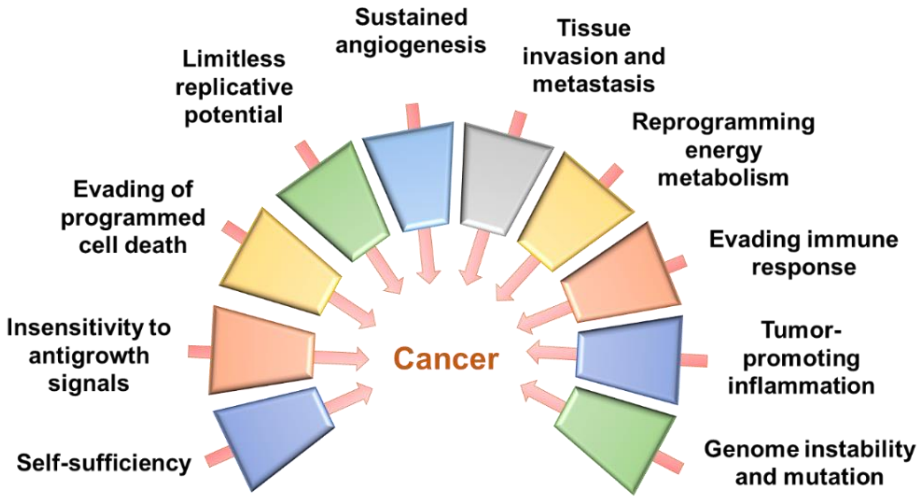

Figure 1. The hallmarks of cancer defined by Doctors Hanahan and Weinberg. *Adapted from [10].*

Although these hallmarks summarize the main known characteristics and biological information about cancer, it is fundamental to understand that cancer is not a single disease and that these characteristics are variable among different tumors. This overview of the hallmarks of this disease provides only a general view to recognize the biology of cancer, identify possible therapeutic targets and contribute to understanding why cancer treatment is complicated [14, 15].

2. Breast cancer

2.1. Epidemiology

Breast cancer (BC) is the second most common cancer worldwide and the most frequent cancer among women in developed and underdeveloped nations, with slightly more cases in underdeveloped than in developed nations. In 2012, 1.67 million of new cases were diagnosed, and 522.000 women died from BC. Not surprisingly, breast cancer is the most prevalent cancer in Portuguese women (**Figure 2**), with 6088 new cases diagnosed every year and with an incidence rate of 67.6 cases per 100.000 people [4].

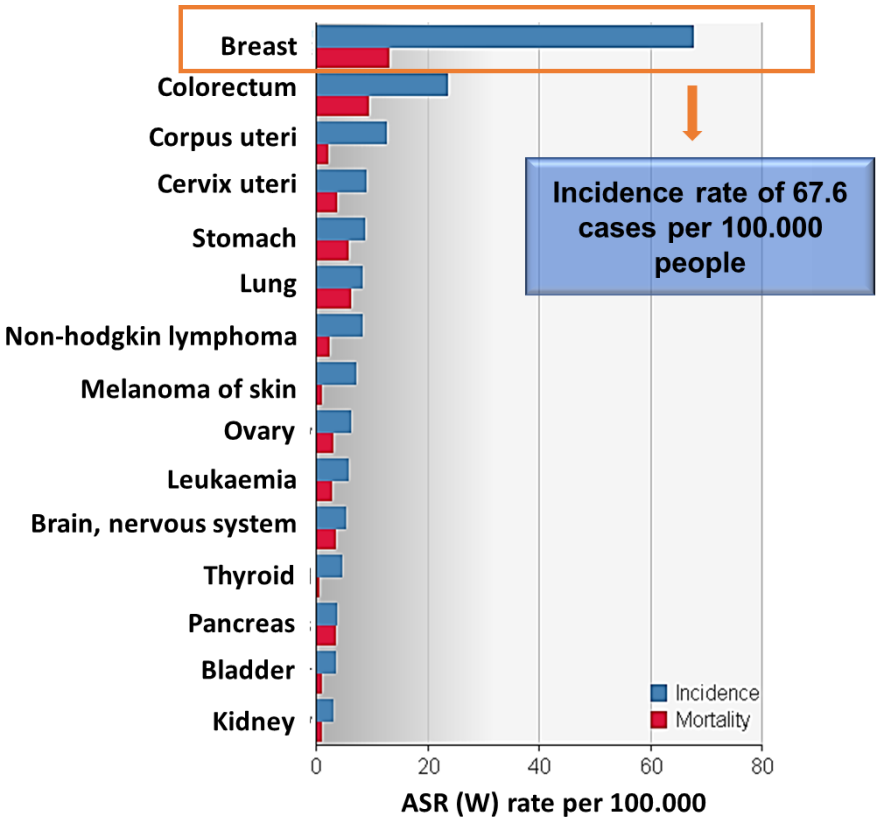

Figure 2. Globocan estimations for 2012 regarding the incidence and mortality rates of the most common types of cancer in women, in Portugal. *The age-standardized rate (ASR) of breast cancer incidence is 67.6 per 100.000 people. Adapted from [4].*

The differences in cancer incidence, mortality and survival rates worldwide are related to different risk factors, accessibility to screening programs and effective treatments [16]. A relevant risk factor for BC (as for all other cancers) is age, being more prevalent in the 45-65 years old age group [17]. Besides that, other risk factors include family history of breast cancer (such hereditary germline mutations in the BC susceptibility genes *BRCA1* and *BRCA2*), reproductive events (early menarche, late pregnancies, lactation and late menopause - due to a higher exposure to elevated levels of hormones), sedentary lifestyle, alcohol consumption and exogenous hormone use [18].

Portugal initiated its first BC screening program back in 1990. Nowadays, the implemented BC screening program offers digital mammograph to women aged between 45-69 years old. The incidence rate of BC in Portugal is currently higher than the mean for other European Union countries [17, 19].

2.2. Molecular subtypes of breast cancer

BC is a complex and heterogeneous disease. This heterogeneity affects the therapeutic response and disease progression [20]. Therefore, the categorization of tumors has an important role to select the best treatment and patient care, since different treatments exist which can only be effective in a selective type of BC [21].

Genomic analysis have provided new insights to better understand breast carcinomas [22]. Perou *et al*. (23) and Sorlie *et al.* (24) established that BC could be classified based on global gene expression. They classified breast tumors into four main groups (**Table 1**): Luminal A, Luminal B, human epidermal growth factor receptor (HER)-2 enriched and Triple negative (**Figure 3**) [23, 24]. Nevertheless, as genomic studies evolved, different intrinsic subtypes have emerged such as the Claudin-Low subtype [25].

Table 1. Characteristics of molecular subtypes of BC. *Adapted from [26].*

Molecular subtype	ER	PR	HER-2	Basal markers
Luminal				
Luminal A	+	+	-	-
Luminal B	+	+/-	+/-	+/-
HER-2 enriched	+/-	+/-	+	+/-
Triple negative	-	-	-	+

ER, estrogen receptor; PR, progesterone receptor; HER-2, human epidermal growth factor receptor 2.

Luminal breast cancers are the most common subtype of BC (more than 75%). These tumors are characterized by the relatively high expression of luminal markers such as progesterone receptor (PR) and estrogen receptor (ER) and they usually have a better prognosis [21]. Luminal BC is divided into **Luminal A** and **Luminal B,** due to different prognosis, different gene expression levels and treatment response. Luminal A BC are characterized by PR and/or ER positive and HER-2 negative. These are the most common subtype and are associated with a less aggressive phenotype when compared with luminal B tumors. Luminal B BC have a lower or no PR expression and lower expression of ER, and may present HER-2 overexpression, presenting a worse prognosis [20, 27].

Nevertheless, luminal tumors show better outcomes and a broader range of treatment options when compared with other types of BC.

HER-2 overexpressing tumors represent approximately 10-15% of BC and have high levels of the HER-2 receptor, a tyrosine kinase receptor which is involved in regulation of cellular growth. These tumors do not express hormone receptors (ER and PR) and are associated with poor prognosis (higher rates of recurrence and mortality) [21]. However, patients treated with monoclonal antibodies against HER-2 (targeted therapy) have shown good clinical responses [28].

Triple-negative breast cancer (TNBC) is the most heterogeneous group among all subtypes. It represents 15-20% of all breast cancers and is characterized by the lack of expression of PR, ER and HER-2. Usually, these tumors have an aggressive phenotype, high histologic grade and high levels of proliferation and invasion, with an extremely poor prognosis and shortest survival [29]. TNBC have the greatest intrinsic diversity, being composed by distinct molecular subtypes that respond differently to current therapies [30]. Six molecular subtypes of TNBC were identified (**Figure 3**): basal-like 1 (BL1), basal-like 2 (BL2), mesenchymal (M), mesenchymal stem-like (MSL), luminal androgen receptor (LAR) and immunomodulatory (IM) [31].

Both **BL1** and **BL2** subtypes are enriched in components and pathways of cell cycle and cell division. In particular, **BL1** have high expression of cell cycle and DNA damage response genes, presenting increased proliferation (due to the increased ki-67 mRNA expression and the enrichment in proliferation genes). Patients with this subtype of TNBC could respond to antimitotic agents (e.g. taxanes such as docetaxel and paclitaxel). The **BL2** is characterized by an enrichment in myoepithelial markers and in growth factor receptor genes expression (MET, EGFR and EPHA2). This subtype has high expression of Membrane Metalloendopeptidase (MME) and TP53, which are suggestive of basal/myoepithelial origin [31, 32].

The **mesenchymal** subtype is enriched in genes involved in the epithelial to mesenchymal transition (EMT), extracellular matrix interaction and cell motility. Since these cells have activated PI3K/AKT signaling, these cancer cells may be sensitive to mTOR inhibitors. They may also respond to eribulin mesylate, a drug that suppresses the EMT transition pathway [32, 33].

The **MSL** subtype is also enriched in genes involved in the EMT and in growth factor genes. These tumors express low levels of proliferation genes and present high expression of genes associated with stem cells [32, 33].

The most distinct subtype among TNBC is the **LAR**. These tumors are ER negative but are enriched in hormone regulation pathways including androgen/estrogen metabolism, steroid synthesis and porphyrin metabolism [33, 34].

The **IM** subtype is mainly composed by genes involved in immune cell and cytokine signaling, and in core immune signal transduction pathways [32] Compared with other subtypes, these patients show a better treatment outcome [33, 34].

Additionally, a **claudin-low** subgroup has been described. The **Claudin-Low** is mainly composed of the M and MSL subtypes and is characterized by the low expression of claudin proteins that are involved in tight junctions and epithelial cell-cell adhesion, namely claudins 3, 4 and 7, cingulin, E-cadherin and occludin. These tumors also show low expression of luminal markers, high expression of EMT markers, and they are enriched in cancer stem-cell-like features such as low expression of the epithelial differentiated marker CD24, and high expression of CD44 and aldehyde dehydrogenase 1 (ALDH1) [25, 35, 36]. These tumors are clinically associated with a poor prognosis and are relatively resistant to conventional chemotherapy [37].

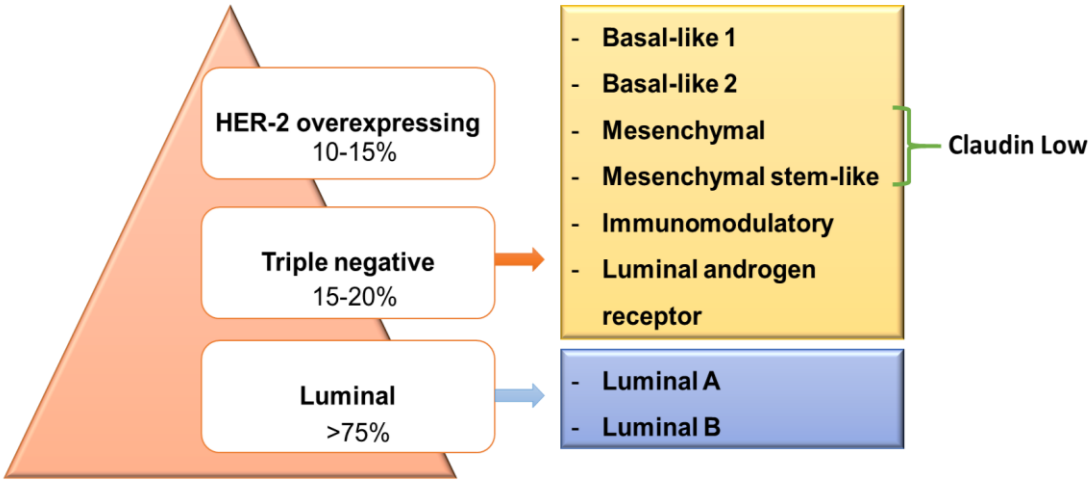

Figure 3. Molecular classification of triple negative breast cancer. Adapted from [26, 32]

2.3. Breast cancer stem cells

Accumulating evidence suggests that different cancers have one characteristic in common: the heterogeneity among cancer cells within a single tumor. Without exception, BC comprises a heterogeneous tumor cell population with multiple subtypes, different gene expression patterns, and different clinical outcomes. This heterogeneity could be explained by two major theories, the clonal evolution model and the cancer stem cells hypothesis.

According to the **clonal evolution model** (**Figure 4**), random cells can acquire different mutations that provide a selective growth advantage comparing with normal cells, leading to a clonal expansion. This dominant population has uncontrolled proliferation and tumorigenic potential. The heterogeneity is due to the acquisition of new mutations that can provide growth advantages over other tumor cells. Besides the acquisition of genetic events, clonal expansion could be also triggered by different epigenetic mechanisms and by microenvironmental changes [1, 2].

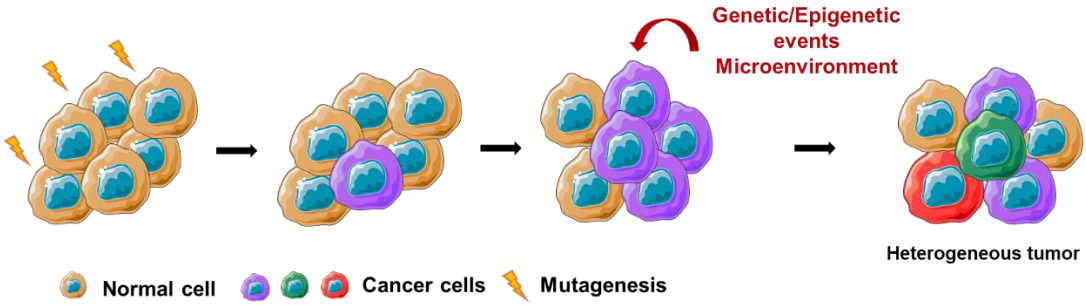

Figure 4. The clonal evolution model. *Any normal cell can be the target of transformation. Mutated cells can acquire additional mutations giving rise to an heterogeneous tumor. Adapted from [1].*

According to the most recent model, the **cancer stem cells hypothesis** (**Figure 5**), only a small population of tumor cells, with stem characteristics, has the capacity of self-renewal and differentiation. These characteristics give rise to the different cells that comprise a tumor and, consequently, to tumor heterogeneity [1, 38].

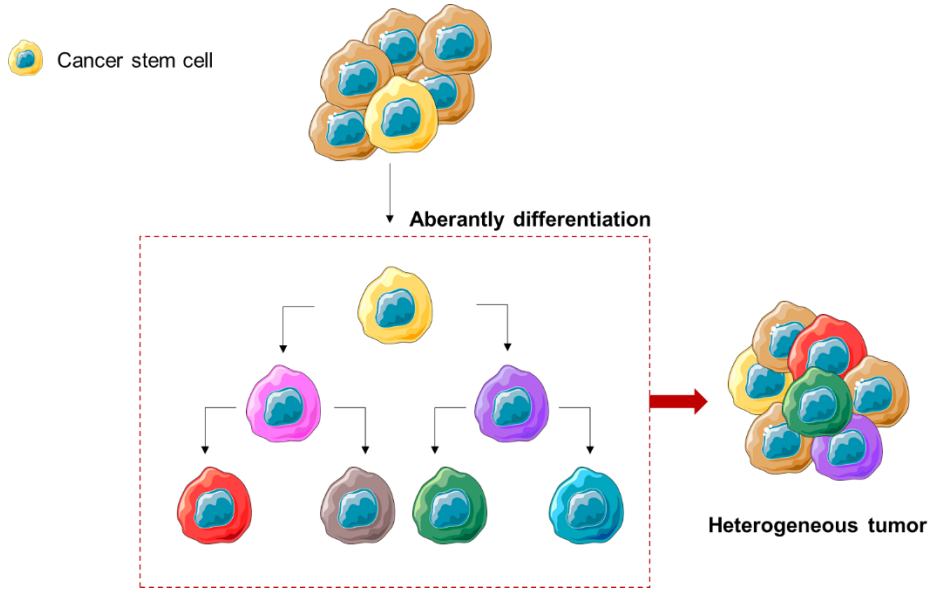

Figure 5. The cancer stem cell hypothesis. *Only a small population of cells with stem characteristics can propagate a tumor, based on their self-renewal and differentiation capacity. Adapted from [1].*

It is currently believed that these two different models are not mutually exclusive and some aspects are not clearly addressed by them. For example, a single CSC is not capable of reconstituting a whole solid tumor when injected in immunocompromised mice, which puts in question the cancer stem cell hypothesis [39]. Therefore, it is now believed that tumor heterogeneity could be caused by a combination of these two models [1].

2.3.1. Characteristics of CSCs

CSCs are a small population of cells within a tumor categorized by their capacity of self-renewal and differentiation, having high proliferative potential, therefore playing an important role in the tumor formation and growth [40].

CSCs may arise either from differentiated cells or from normal stem cells that acquire oncogenic mutations that make them malignant cells with stem characteristics. These cells can divide symmetrically, i.e. originating identical stem cells with the same self-renewal capacity, or they can divide asymmetrically, resulting in one stem-cell and one differentiated progenitor cell [40].

CSCs are frequently associated with cancer treatment failure, tumor metastasis and recurring lesions after treatment. Besides that, they have a high resistance to radio- and chemotherapy, and metastatic activity [38].

The resistance of CSCs to chemotherapeutic agents and radiation is a significant clinical problem, since remaining resistant CSCs may lead to recurrence of the disease. Therefore, the search for specific molecular targets and the development of more effective treatments are fundamental to eliminate CSCs [41].

2.3.2. Signaling Pathways Involved in CSC Maintenance

CSCs have the capacity of self-renewal and differentiation. However, since these cells represent a small population within a tumor, it remains difficult to effectively study the molecular pathways involved in CSCs maintenance [42]. The following pathways have been suggested to be involved in CSCs maintenance, thus being possible targets for CSC therapies:

p53 Pathway

In normal cells, the p53 induces cell cycle arrest, senescence or apoptosis preventing the multiplication of cells with genetic mutations. This gene is mutated in a high proportion of human cancers (more than 50%). The loss of the tumor suppressor gene *p53* promotes an accelerated cell proliferation and malignant transformation. Recent studies have demonstrated the effects of *p53* loss or mutation on the CSCs population. In BC cells, the *p53* loss can lead to an inhibition of differentiation, thus enabling cells to acquire stem cell properties. Therefore, restoring *p53* function remains an attractive approach to target the CSC population in BC [43, 44].

Notch Signaling Pathway

Notch receptors are involved in different biological functions, such as cell differentiation, proliferation, migration and apoptotic events [42]. The notch signaling pathway is complex and multifaceted and is implicated in cellular communication through transmembrane ligands and receptors. This pathway plays a critical role in CSCs self-renewal and angiogenesis regulation [45]. This pathway is also usually deregulated in cancer, including in BC. Recent studies have shown that the inhibition of Notch signaling by γ-secretase inhibitors (antagonists of Notch signaling), reduced sphere formation (which develops from the proliferation of CSCs) and proliferation, and significantly reduced CSC activity [46, 47].

Wnt/β-Catenin Signaling Pathway

The Wnt/β-Catenin signaling pathway regulates cell proliferation and differentiation, migration and asymmetric cell division. This pathway leads to the activation of β-catenin, which accumulates in the nucleus inducing the expression of Wnt target genes.

Wnt/β-Catenin signaling is frequently aberrantly activated in a vast number of cancers, promoting the survival and growth of CSCs [46].

Hedgehog Signaling Pathway

The Hedgehog signaling pathway is involved in the repair of normal tissues, stem-cell maintenance, tissue-patterning during embryonic development and epithelial-to-mesenchymal transition [48]. Different cancers present aberrant Hedgehog signaling. In particular, members of this pathway (Gli1, Gli2 and PTCH1) are highly expressed in breast CSCs [49].

2.3.3. Breast Cancer Stem Cells Surface Markers

The characterization and isolation of CSCs represent an important approach in cancer research with significant therapeutic implications. Even so, the identification of molecular markers of CSCs remains a challenge due to their similarity to normal stem cells and the limited number of CSCs in tumor tissues and cell culture.

The most frequent combination of markers used to determine breast CSCs includes CD24, CD44 and ALDH1 (**Figure 6**) [50, 51].

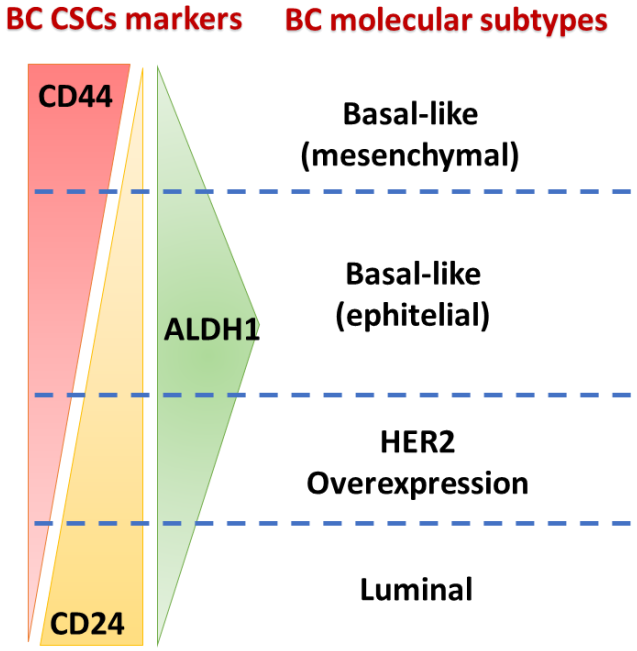

Figure 6. Expression of stem cell markers in different breast cancer (BC) molecular subtypes. *Adapted from [52].*

CD44

CD44 is a transmembrane glycoprotein which has an important role in cell adhesion, angiogenesis, motility, proliferation, differentiation and cell survival. It is also involved in signaling cascades where CD44 interacts with neighboring receptors (i.e. tyrosine kinases) enhancing tumor initiation. This glycoprotein, as a specific receptor for hyaluronic acid (HA), promotes migration both in normal and malignant cells. It can be up-regulated in a broad range of tumors such as breast, melanoma, cervix, lung and ovarian [50].

CD44 is an important surface marker on CSCs and its high expression is related with poor prognosis and higher tumorigenicity and metastatic potential. CD44 can interact with P-gp (P-glycoprotein) promoting cell invasion and migration of tumor cells and, by

transmitting survival and anti-apoptotic signals, it can also induce multidrug resistance in CSCs [50, 53]. Furthermore, in breast and ovarian tumors, the interaction of Nanog, a transcription factor implicated in self-renewal of undifferentiated embryonic stem cells, with HA and CD44 can lead to the appearance of Rex1 and Sox2 that are stem cell regulators [50].

It has been shown that $CD44^+$ cells promoted tumorigenesis of BC cells displaying stem cell properties [50, 54]. Al-Haji et al. recognized CD44+/$CD24^{-/low}$ cells as probable CSCs from the basal/mesenchymal breast cell lines MDA-MB-231 and MCF-7; this was later supported by other authors [55-57].

Aldehyde dehydrogenase 1 (ALDH1)

Aldehyde dehydrogenases (ALDHs) are a family of $NAD(P)^+$-dependent enzymes comprised of 19 isoforms that are localized in the mitochondria, cytoplasm or nucleus. The aldehydes are crucial in physiological processes (e.g. vision, embryonic development and neurotransmission). However, most of them are cytotoxic and need to be detoxified, therefore, ALDHs exert important functions in aldehyde detoxification (by oxidizing the aldehydes to their respective carboxylic acids), in ester hydrolysis [serving as binding proteins for different endogenous (e.g. androgen and cholesterol) and exogenous (e.g. acetaminophen) compounds], and in antioxidant functions [by the production of NAD(P)H, hydroxyl radicals scavenging and ultraviolet light absorption] [58, 59].

Among the ALDH superfamily, the high activity of the isoenzyme ALDH1 has been shown to be an eligible marker of stemness in BC and it is believed to contribute to the early differentiation of stem cells. ALDH1 is a multifunctional enzyme responsible for the oxidation of endogenous and exogenous aldehydes to their equivalent carboxylic acids [50, 51]. ALDH1 expression is considered a predictive factor for early metastasis and decreased survival in BC patients. Genistier *et al.* demonstrated that normal and malignant human breast epithelial cells with high activity of ALDH1 show stem cell properties [51].

In BC, CSCs were identified and isolated for the first time by Muhammad *et al*. Using a model in which human BC cells were grown in immunocompromised mice, they verified that only a minority of cells have the ability to form new tumors. They characterized these cancer cells based on cell surface marker's expression and identified these cells as $CD44^+/CD24^{-/low}$ Lineage [55]. However, this CSC phenotype is not universal and other options have been

proposed to better identify breast CSCs, particularly in TNBC. This BC subtype is mainly composed of cells expressing CD44 and high activity of ALDH1 [51, 60].

Therefore, the $CD44^+/ALDH1^{high}$ phenotype has been proposed to identify and isolate breast CSCs. Cells with this phenotype have high tumorigenic ability, high metastatic propensity and they are resistant to conventional cancer therapies [61].

Indeed, different studies show that the $CD44^+/ALDH1^+$ population has enhanced metastatic capacity both *in vitro* and *in vivo*. In addition, cells with this phenotype were more resistant to different chemotherapeutic drugs [61]. Besides that, an increased expression of Wnt/ β-catenin and Notch signaling pathways has been found in BC cell lines having this phenotype [62]. These findings support the idea that the $CD44^+/ALDH1^+$ phenotype could be a good approach to identify and isolate breast CSCs.

2.3.4. Future perspectives in therapy

Currently, conventional cancer therapies frequently lead to treatment failure and tumor relapse, due to resistance of cancer cells to chemo- and radiotherapy. CSCs are believed to be the main responsible for this resistance. Therefore, the elimination of CSCs is crucial to achieving complete eradication of cancer cells [63].

Different new therapeutic systems have been proposed to target CSCs and to modify the microenvironment (niches) that supports these cells.

One of these strategies consists in directly attacking CSCs by targeting cellular surface markers, which will then cause apoptosis, senescence or terminal differentiation. The development of monoclonal antibodies to target CSCs has acquired a great attention. Marangoni *et al.* showed that targeting CD44 with an anti-CD44 antibody (P245) inhibited the growth of BC xenografts in nude mice [64].

Targeting ATP driven efflux transporters has been proposed as another strategy to eliminate CSCs. Indeed, CSCs overexpress drug transporter proteins which can cause an efflux of various chemotherapeutic drugs, leading to various treatments failure. The ATP-binding cassette (ABC) superfamily includes three principal multidrug resistance genes: ABCB1 (P-glycoprotein 1), ABCG2 (BCRP1) and ABCC1 (MRP1). In this way, the inhibition of these proteins could increase the response of CSCs to chemotherapeutic agents [65].

Targeting key signaling cascades is another strategy against cancer stem cells. Indeed, some signaling pathways are deregulated in CSCs, such as the Hedgehog, Wnt/β-catenin and Notch. Some signal molecules from the CSC regulation pathways or downstream signal molecules could be potential targets for CSCs therapy [65]. Some of these agents are under investigation in phase I and II of clinical trials and some have reached the clinic. For

example, a Hedgehog inhibitor, the Vismodegib, was approved for basal cell carcinoma treatment in 2012. Different monoclonal antibodies and Notch inhibitors such as γ-secretase have been studied. In particular, the monoclonal antibody Tarextumab, which is currently in phase II clinical trial [66].

Finally, the last strategy is to attack the tumor microenvironment, which provides a niche for CSCs maintenance. The CSC niche is comprised by a bulk of cancer cells, stromal fibroblast, hematopoietic, endothelial and vascular cells. This niche can directly affect the drug sensitivity and mobilization of CSCs, thus, it could be a target for CSC-directed therapy. Tumor blood vessels constitute the major component of the vascular niche which is regulated by the vascular endothelial growth factor (VEGF). One possible approach to attack the CSC niche is by inhibiting angiogenesis with Bevacizumab, a neutralizing antibody of VEGF that blocks endothelial cell migration and tube formation [41, 66].

These strategies provide new promising opportunities to effectively treat tumors without recurrence and treatment failure. The better understanding of CSCs biology is fundamental to achieve the goal of eliminating the CSC population [66].

3. Natural products and extracts and their application in cancer treatment

Cancer treatment typically involves surgery, radio- and chemotherapy. More recently, hormonal and target therapy have been discovered.

In BC, chemotherapy is the main approach for treatment, mainly in metastatic tumors, and typically involves a combination of different drugs or a drug that affects different targets [67, 68]. Not surprisingly, these approaches exhibit numerous side effects in patients. They can induce cell toxicity, liver and kidney damages, neurotoxicity or, bone marrow suppression. Moreover, the drugs used in chemotherapy can affect not only the cancer cells but also the non-tumor cells, therefore inducing genotoxic, carcinogenic and teratogenic effects in normal cells [67, 69].

On this point, natural products have gained attention in the field of cancer treatment due to their availability and since they are a source of bioactive compounds, many of them having antitumor potential. Natural products have been used to treat several diseases for decades and, more recently, different studies have revealed some natural products with interesting antitumor properties [70].

In the last years, an important proportion of the anticancer drugs used in the clinic are synthetic derivatives or analogues from phytochemicals initially discovered on teas, spices or medicinal plants known to have antitumor potential [7].

In fact, there is a continuous need to search for new, powerful and natural antitumor agents causing low side-effects (not affecting the non-tumor cells), while capable of inhibiting tumor cell proliferation pathways [71]. In addition, there is lack of knowledge on the effect of natural compounds on CSCs and therefore their potential as CSCs inhibitors has not been thoroughly investigated.

3.1. Eucalyptus

The genus *Eucalyptus* belongs to the Myrtaceae family and it is native from Australia. Nowadays different species of *Eucalyptus* are distributed around the world and they are largely cultivated to produce paper, cellulose, timber, charcoal, and pharmaceuticals, corresponding to one-third of the total forest area in Portugal [72].

Regarding the medicinal uses, *Eucalyptus* is traditionally used to produce essential oils for either cosmetics or pharmaceuticals. In addition, it is used for herbal preparations to treat colds, pain, influenza, chest problems, fever and inflammation [69, 73].

The genus *Eucalyptus* is an abundant source of phytochemicals and studies have shown that some extracts and components from *Eucalyptus* possess cytotoxic and antiproliferative effects in different tumor cells (from breast, liver, leukemia and cervix) [74, 75]. *Eucalyptus* contains high levels of volatile organic compounds, mostly the monoterpene 1,8-cineole, known as eucalyptol, which was associated with anticancer effects [75]. Regarding the nonvolatile compounds, such as resveratrol, piceatannol, and macrocapal G, they also have cytotoxic and growth inhibitory activity against human breast, colon, ovary, liver, prostate, neuroblastoma, cervix, lung and gastric cancer cell lines. However, it is important to note that the part of the plant from which the extract was prepared, the extraction method and the extraction solvent affect the cytotoxic activity of the extract. Additionally, the plant species, location, extraction season and conditions, and sample preparation method affect the extraction efficiency of the bioactive compounds [73]. To our knowledge, there are no studies on the effect of Eucalyptus extracts on CSCs.

3.2. Melissa Officinalis

Melissa officinalis L. (lemon balm) is a member of the Lamiaceae family, originally native of the Western Asia and Eastern Mediterranean region. *Melissa* is the most used medicinal

plant in Europe and Mediterranean region. In Portugal, *Melissa officinalis* is known as “erva-cidreira” and it is commonly used as an herbal tea due to its digestive, aromatic, sedative and antispasmodic properties [76, 77].

M. officinalis possesses antibacterial, antifungal and anti-inflammatory effects and can be also used as an expectorant, and for the treatment of headaches and rheumatism. Recently, some studies have reported its antioxidant, antiproliferative and antitumor effects [78, 79].

The main components of *M. officinalis* are polyphenolic compounds, including essential oils (e.g. citronellal), caffeic acid derivatives (e.g. rosmarine acid, which corresponds to the most abundant phenolic compound), flavonoids and quinic acid, γ-tocopherol, fructose and glucose [79].

Some studies have evaluated the antitumor activity of *Melissa* extracts in some human tumor cell lines. It has been found that 72h treatment with this extract can reduce cell proliferation to approximately 40% in human colon cancer cells. This effect may be due to the high quantity of rosmarinic acid found in *M. officinalis [80].* Furthermore, it has also been demonstrated that this extract affects the cell cycle profile of non-small cell lung cancer cells and induces their cell death by apoptosis [78].

Therefore, *M. officinalis* is a source of bioactive compounds which may have antitumor activity in a broad range of tumors. To our knowledge, there are no studies on the effect of *M. officinalis* extracts on CSCs.

3.3. Curcumin

Curcumin (1,7-bis(4-hydroxy- 3-methoxyphenyl)-1,6-heptadiene-3,5-dione), from now abbreviated a CUR for simplicity, is a hydrophobic polyphenol present in the rhizome of Turmeric (*Curcuma longa).* Traditionally, Turmeric has been used in food flavoring, fabric coloring and medicinal applications particularly as an anti-inflammatory agent [81, 82]. From the innumerous bioactive compounds isolated from Turmeric, CUR has been found as the compound presenting the greatest bioactivity [82].

CUR possesses antioxidant, antibacterial, anti-inflammatory and anti-amyloid properties. In addition, there is strong evidence that CUR can be a potential anticancer agent. It has protective and therapeutic efficacy towards a broad range of tumors such as breast, lung, pancreas, colorectal, skin and others [68, 83].

3.3.1. Antitumor and anticarcinogenic effects of curcumin

CUR can, directly or indirectly, interact with several molecules through covalent or non-covalent hydrophobic bonding or hydrogen bonding. The molecular targets include enzymes, tumor suppressors, oncoproteins, transcription factors, inflammatory mediators and carrier proteins.

CUR can modulate different steps of molecular carcinogenesis. Some of them are described below:

Growth inhibition effect: CUR inhibits the growth of different cancer cells, without affecting normal cells, by modulating cell signaling pathways (i.e. Notch, Wnt, Hedgehog) [68].

Induction of apoptosis: CUR can induce apoptosis through the p53-dependent pathway. It can also promote apoptosis by changing the mitochondrial membrane, reducing glutathione and increasing the reactive oxygen species (ROS) levels [68].

Induction of senescence: CUR can inhibit the telomerase expression, which is activated in the majority of cancer cells. Telomerase is responsible for the maintenance of telomere length; thus, the inhibition of telomerase expression leads to cell cycle arrest and cell death [68].

Inhibition of tumor angiogenesis: Some studies revealed the efficacy of CUR as a potent anti-angiogenic, anti-metastatic and anti-invasive agent, through the modulation of STAT3 (Signal transducer and activator of transcription 3), NF-κB (nuclear factor kappa B**)**, MMPs (matrix metalloproteinases) and RhoA (Ras homolog gene family, member A) signaling pathways [68].

Modulation of cell proliferation and regulation of cell cycle: The expression of cyclins and cyclin-dependent kinases (CDKs), which drive the cell through the cell cycle, is frequently aberrant in cancer cells. In BC, CUR can down-regulate cyclin D, the transcription of NF-κB and MMP-1 and it can cause cell cycle arrest in the G2/M phase. It has also been reported that CUR can inhibit the expression of some Wnt/β-catenin pathway components in BC, e.g. the cyclin D1 [68, 84].

Modulation of miRNAs: MicroRNAs (miRNAs) are short non-coding RNAs that regulate the expression of several genes. Several miRNAs have been found deregulated in different tumors. In BC, CUR upregulates the miR-15 and miR-16, thus reducing Bcl-2 expression

and causing cell death. It has been described that CUR can also upregulate the miR181b in metastatic BC cells, leading to inhibition of metastasis [68].

Altogether these characteristics underlie the potential therapeutic effects of curcumin against cancer [68]. In addition, there are several studies on the potential of CUR to target CSCs, as described next.

3.3.2. Regulation of CSC self-renewal pathways by CUR

Several studies have shown that CUR can target CSCs by affecting their self-renewal pathways. As described above (section 2.3.2.), and the Hedgehog, the Notch and the Wnt/β-catenin signaling pathways, among others, have an important role in CSC self-renewal.

Regarding the Wnt/β-catenin signaling pathway, some studies showed that CUR can reduce the β-catenin levels. It can induce caspase-3-mediated cleavage of β-catenin, which leads to the inactivation of this signaling pathway. It has also been reported that CUR can down-regulate a positive regulator of the Wnt/β-catenin signaling, the p300 [85].

Regarding the Notch signaling, CUR can inactivate the transcription of Notch-1 by down-regulation of the Notch-1 mRNA levels. It can also down-regulate the NF-κB and the γ-secretase complex protein levels [85, 86].

In what concerns the hedgehog signaling, Li Y *et al.* demonstrated that CUR can down-regulate the Gli1 expression, a transcription factor that leads to the expression of “stemness genes”. It can also reduce the levels of the transmembrane receptor Patched 1 (Ptch1) [85].

Regarding the mentioned biological effects, CUR remains a promising therapeutic agent against cancer and particularly, against CSCs. Nevertheless, it has poor bioavailability which is related to its low water solubility, low serum levels, rapid metabolism, short half-life and limited tissue distribution. These characteristics constitute important barriers that limit its clinical efficacy [81].

Therefore, research for improving the solubility and stability of curcumin is needed [68].

3.3.3. Strategies to enhance curcumin bioavailability

Different approaches to increase CUR bioavailability have been developed including the preparation of curcumin nanoparticles, liposomal and phospholipid complexes, and polymer micelles, as well as the chemical synthesis of compounds derived from CUR having structural modifications to improve CUR bioavailability [82].

3.3.3.1. Curcumin nanoparticles

Nanoparticles (NPs) are solid and spherical structures ranging around 10-200 nm in size diameter. The particles size influences the biodistribution of NPs and also influences the tissue penetration and cellular uptake of the therapeutic agent. Larger particles might be rapidly taken up by the mononuclear phagocytic system cells and may not penetrate the endothelial barrier [87].

NPs are useful to improve the circulation of the loaded therapeutic molecules such as hydrophilic and hydrophobic small drugs or biological macromolecules. Additionally, targeted-NPs (e.g. with antibodies) also allow to direct the drug to the target organs and control drug delivery. In terms of clinical uses, NPs must fulfill some characteristics such as biocompatibility, proper biodegradation kinetics and drug compatibility [88, 89].

Among the different types of NPs available, polymer nanoparticles are the most attractive for drug delivery, in particular particles prepared from polyesters such as poly(lactide-co-glycolic acid) (PLGA), which is an effective biodegradable polymer approved by the US FDA for drug delivery [89].

PLGA is a copolymer of polylactic acid (PLA) and polyglycolic acid (PGA) and it is considered a prevailing choice in several biomedical devices production, due to its biodegradability and biocompatibility. In the body, PLGA suffers hydrolysis to produce lactic and glycolic acid (biodegradable metabolite monomers, **Figure 7**), which are easily metabolized by the Krebs cycle and are removed as water and carbon dioxide; consequently, the systemic toxicity of PLGA is minimal. This type of NPs carry a negative surface charge that promotes particle's stability in circulation [89, 90].

The biodegradability of PLGA is affected by the particle size, shape and morphology, presence of low molecular weight compounds such as oligomers and monomers, method of preparation, the inherent properties of the polymer (e.g. hydrophobicity, molecular weight and chemical structure), mechanisms of hydrolysis, site of implantation and

physicochemical parameters such as pH and temperature [89]. Generally, the more hydrophilic, lower molecular weight, higher glycolide content and more amorphous polymers, the shorter will be the degradation time [91].

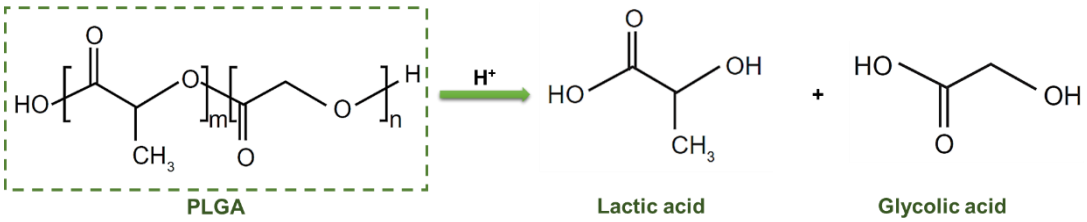

Figure 7. Hydrolysis of poly(lactide-co-glycolic acid) to lactic and glycolic acid. *m and n indicate the number of times each unit is repeated.*

Due to the presence of carboxylic end groups, PLGA-NPs have a negative surface charge at neutral pH. PLGA NPs are internalized in cells via endocytosis and, under the endo-lysosomes acidic pH, they undergo surface charge reversal that facilitates their interaction with the vesicular membranes, which leads to destabilization of the membrane allowing the escape of NPs into the cytosol [92].

The structural organization of the NPs is dependent on the method of preparation [93]. Different preparation methods of NPs have been established: nanoprecipitation, emulsification solvent diffusion, emulsification solvent evaporation and emulsification reverse salting-out. For the encapsulation of hydrophobic molecules (e.g. curcumin), the common method used is the nanoprecipitation technique, a one-step procedure, also known as the solvent displacement method. In this method, the polymer and drug are dissolved in a polar solvent. The solvent should be miscible in water, organic and easily removed by evaporation (e.g. acetone). This solution is dropwise added, under magnetic stirring, into an aqueous solution with a surfactant which allows the rapid formation of the NPs by solvent diffusion [89, 91].

Curcumin-loaded NPs present great promise as anticancer chemotherapeutic agents, protecting CUR from degradation and increasing their stability. Moreover, NPs should allow sustained and more efficient CUR release [94].

Aims of the work

The specific aims of the present work were to:

I. Analyze the antitumor activity of natural extracts/compounds (*Melissa Officinalis L.*, *Eucalyptus globulus L. and Curcumin)* in human breast cancer cell lines

II. Develop Curcumin loaded PLGA nanoparticles

III. Analyze the antitumor activity of the Curcumin loaded PLGA nanoparticles in human breast cancer cell lines

IV. Characterize and isolate breast cancer stem cells (CSCs) from the Hs 578T cell line

V. Evaluate the cytotoxic effect of Curcumin and Curcumin encapsulated PLGA nanoparticles in Hs 578T breast cancer stem cells

Materials and Methods

1. Cell lines and cell culture

Two human breast carcinoma cell lines were used for this project **(Table 2)**: Hs 578T (kindly provided by Dr João Nuno Moreira, CNC, University of Coimbra, Portugal) and BT-20 (kindly provided by Dr Joana Paredes, i3S, Porto, Portugal).

Table 2. General characteristics of the Hs 578T and BT-20 cell lines. *Adapted from (26, 95)*

	Molecular subtype	Immunoprofile	Morphology	Disease
Hs 578T	Claudin-low	ER^-, PR^-, $HER2^-$, claudin-3, claudinin-4 and claudinin-7 low	Epithelial	Breast carcinoma
BT-20	Basal-Like	ER^-, PR^-, $HER2^-$	Epithelial	Breast carcinoma

The MKN-45 cell line (gastric adenocarcinoma, kindly provided by Dr Celso A. Reis, i3S, Porto, Portugal) was used as positive control for ALDH1 expression.

The cell lines were maintained in RPMI-1640 with Ultraglutamine I and 25 mM HEPES (Lonza, Basel, Switzerland) supplemented with 10% heat inactivated fetal bovine serum (FBS, Biowest, Florida, USA), from now on named as “complete culture medium with 10% FBS”, except for the Sulforhodamine B (SRB) colorimetric assay where the medium was supplemented with 5% FBS, from now on named as “complete culture medium with 5% FBS” and for the study of the potential cell growth inhibitory activity of CUR and CUR-loaded PLGA nanoparticles in sorted Hs 578T stem-like cells, where medium was supplemented with 20% FBS. Cells were kept at 37°C in a humidified incubator with 5% CO_2.

The Trypan Blue (Sigma Aldrich, St. Louis, USA) exclusion assay was used to determine the cell concentration and cell viability before all experiments. The assay is based on the principle that viable cells possess intact cell membrane that exclude the dye (Trypan Blue), whereas the non-viable cells possess compromised membrane and incorporate the dye.

In this assay, the cell suspension was mixed with the Trypan Blue solution (0.2%) in a 1:1 ratio and then loaded into a Neubauer chamber for cell counting using a bright-field inverted microscope. Cell concentration was calculated by as follows:

$$Cell\ concentration = \frac{Number\ of\ viable\ cells * dilution\ factor * 10^{4\ (*)}}{Number\ of\ Neubauer\ chamber\ quadrants\ analysed}$$

(*) The volume of each corner of the Neubauer chamber is 1 x 10^{-4} mL. Therefore, it is necessary to multiply by 10^4 to obtain the number of cells per mL.

Cell viability was calculated as follows:

$$Cell\ viability\ (\%) = \frac{Number\ of\ viable\ cells}{Total\ number\ of\ cells}$$

All assays were performed only with cells having % viability higher than 90%.

2. *Eucalyptus globulus L. and Melissa officinalis L.* extracts: analysis of tumor cell growth inhibitory activity with the Sulforhodamine B colorimetric assay

2.1. Preparation of plant extracts and stock solutions

Two plant extracts were used: *Eucalyptus globulus L.*, extracted by two different methods (infusion and decoction) and *Melissa officinalis L.* extracted by infusion. Both extracts were provided by Prof. Isabel Ferreira, from the Mountain Research Center (CIMO), Polytechnic Institute of Bragança.

Eucalyptus globulus (infusion and decoction) and *Melissa officinalis* (infusion) were dissolved in distilled water to a final stock concentration of 25 mg/mL or 100 mg/mL, respectively. Aliquots of these extracts were prepared and stored at -20°C to avoid repeated freeze-thaw cycles.

2.2. Cell growth inhibition assay: Sulforhodamine B colorimetric assay

The potential cytotoxicity of the extracts in the Hs 578T and BT-20 cells was tested with the SRB colorimetric assay.

For this assay, Hs 578T and BT-20 were used and the optimal density of cells to be plated in the 96 well-plates was determined for 48h assays, as follows.

Serial dilutions of cells (ranging from 1 x 10^4 to 1 x 10^5 cells/mL for the Hs 578T cell line and from 2 x 10^4 to 2 x 10^5 cells/mL for BT-20 cell line) were prepared. A volume of 100 µL of these cells (at the mentioned concentrations) was seeded in a 96 well-plate and cells were maintained at 37°C in a humidified incubator containing 5% CO_2 for 24h. After this time, 100 µL of complete culture medium with 5% FBS were added to mimic the addition of the plant extracts in the subsequent assays. After 48h of incubation, cells were analyzed under standard bright field illumination using a microscope and the cell concentration that ensured an exponential growth of the cells during 48h was selected for the assays.

Therefore, the optimal concentrations (4 x 10^4 cells/mL for Hs 578T cells and 1 x 10^5 cells/mL for BT-20 cells) were used in subsequent assays. For each experiment, a T0 plate (used for control of cell growth, as it only contains medium and cell suspension) and a T48 plate (corresponding to cells treated with the plant extracts for 48 hours) were prepared. Both cell lines were seeded in duplicate wells and, to determine the background absorbance, cell culture medium-only was plated and used as control. Both plates were maintained at 37°C in a humidified incubator containing 5% CO_2 for 24 hours to allow cell attachment. After this time, the T0 plate was fixed with 10% (w/v) ice-cold trichloroacetic acid (TCA, Merck, New Jersey, USA) for 1 hour at 4° C and washed 3 times with distillate water. The cells in the T48 plate were incubated with five serial dilutions of each plant extract for 48 hours. Serial dilutions of the extracts were prepared in cell medium, ranging from 200 to 12.5 µg/mL. Doxorubicin (Sigma Aldrich) was used as a positive control, ranging from 1250 to 78.1 nM for Hs 578T cells and from 150 to 9.38 nM for the BT-20 cells. Additionally, the solvent in which the plant extracts were diluted (distilled water) and the doxorubicin solvent (dimethyl sulfoxide, DMSO) were tested as controls, by treating cells with the maximum used concentration of each solvent. Blank treatment (cells growing in complete culture medium with 5% FBS and without any further treatment) were also used as control. A schematic representation of the T48 96-well plate for the SRB assay is detailed in **Figure 8**.

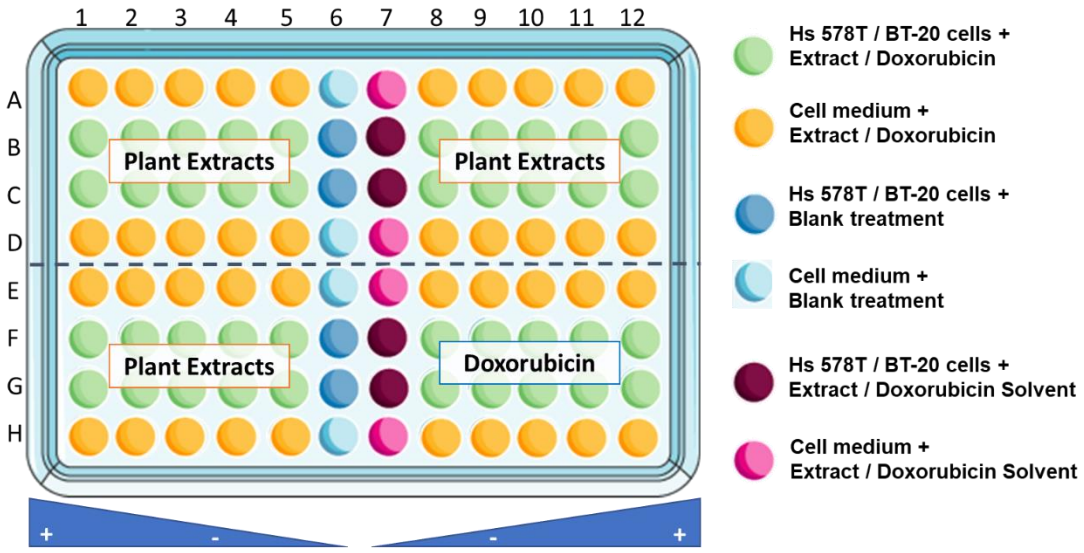

Figure 8. Schematic representation of the T48 96-well plate prepared for the SRB assay. *Cells were plated and 24 hours later 5 serial dilutions of the plant extracts or doxorubicin were added. In column 6 cells were treated with Blank treatment (cell medium) and in column 7 cells were treated with the extract's solvent (distilled water) and doxorubicin solvent (DMSO) as Controls*

After 48 hours of incubation, the T48 plate was fixed as described for the T0 plate and was then washed 3 times with distillate water and allowed to dry at room temperature (RT) overnight (O/N). When completely dry, 50 µL of 0.4% (w/v) SRB (Sigma Aldrich) were added to each well, for both the T0 and the T48 plates, for 30 min. The plates were incubated at RT and then each well was washed 3 times with 1% (v/v) acetic acid (Merck) to remove unbound dye. The plates were left to dry O/N. Finally, to solubilize the protein-bound dye, 100 µL of 10 mM Tris Base (Sigma Aldrich) were added and incubated for 5 min in an orbital shaker. The absorbance was measured at 510_{nm} in a microplate reader (Synergy™ Mx, BioTek Instruments Inc.) and analyzed with the Gen5™ software. The GI_{50} concentrations (the concentrations of plant extracts that cause 50% inhibition of cell growth) were determined for each extract using an Excel datasheet [95]. **Figure 9** is a schematic representation of the workflow.

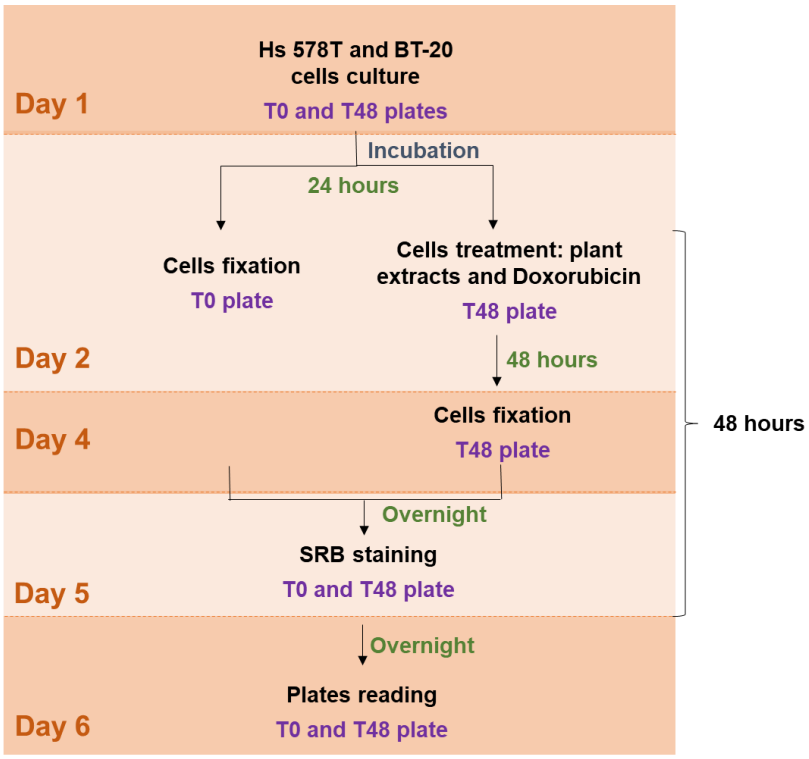

Figure 9. Description of the workflow of the SRB assay.

3. Curcumin loaded into PLGA [poly(lactic-co-glycolic acid] nanoparticles

3.1. Preparation of curcumin loaded PLGA Nanoparticles

In collaboration with Dr. Tiago dos Santos (Post-Doc researcher at the Biomaterials for Multistage Drug & Cell Delivery Group, i3S), curcumin loaded PLGA [poly(lactic-co-glycolic acid] nanoparticles were prepared using the nanoprecipitation technique.

Three different formulations, differing on the initial concentration of curcumin (Sigma Aldrich), were tested: 1 mg, 0.5 mg and 0.1 mg. Briefly, 1.6 mg of curcumin were dissolved in 1.6 mL of acetone (Thermo Fisher Scientific, Waltham, USA; organic phase) to obtain a final concentration of 1 mg/mL. Then, 1 mL, 0.5 mL or 0.1 mL of this solution were added to 20 mg of PLGA (PLGA 5004A, 44 kDa, kindly offered by Corbion, with a 50:50 D,L-lactide:glycolide ratio and 0.4 dL/g viscosity) obtaining a final concentration of 1 mg/mL, 0.5

mg/mL and 0.1 mg/mL, respectively. These solutions were stirred O/N on a magnetic stir plate to get an uniform polymer solution.

These solutions were added drop-by-drop to 0.5% w/v, aqueous phase of 10 mL of Poloxamer 407 (Kolliphor® P407, BASF, Ludwigshafen am Rhein, Germany) using a syringe positioned with the needle (25G) directly in the solution while it was shaken on a magnetic plate (200 rpm). The resulting nanoparticles were stirred at room temperature for 3 hours to evaporate the organic solvent. Blank PLGA nanoparticles were prepared, following the same protocol, by dissolving the PLGA polymer in organic solvent without curcumin.

3.2. Concentration and washing of curcumin loaded PLGA nanoparticles

The three nanoparticles solutions containing 1 mg/mL, 0.5 mg/mL or 0.1 mg/mL of curcumin were concentrated by centrifugation using an Amicon® (Darmstadt, Germany) filtration device with 100 kDa molecular weight (MW) cut off membrane at 3166x *g* for 10 minutes at 4° C. Then, the nanoparticle solutions were washed twice with 10 mL of deionized (DI) water by centrifugation under identical conditions using the Amicon®, to remove larger aggregates, free polymer and free curcumin. The filtered fluids were rejected between centrifugations, 10 mL of freshly DI water were added and nanoparticles were resuspended using a micropipette. The resulting nanoparticles (Nano-CUR) were resuspended in 1.5 mL of DI water and stored at 4° C until being tested.

3.3. Characterization of Nano-CUR formulations: Particles Size and Zeta Potential

The nano-CUR particles were analyzed using the Zetasizer (Nano ZS, Malvern Instruments, Malvern, UK) to obtain the size of the particles, its polydispersity index (PDI), and charge.

The nano-CUR particles were diluted (1:100) in 1 mL of DI water. These suspensions were placed into a disposable folded capillary cell (DTS1070, Malvern) using a syringe. The mean diameter of nanoparticles and Zeta Potential, together with the polydispersity index, were obtained from the analysis of 3 runs of each sample. The measurements were performed at 25 °C and the results were obtained with the Zetasizer software v7.12.

3.4. Determination of CUR encapsulation efficiency

The amount of curcumin incorporated into the nanoparticles was determined by a direct method, using a UV-VIS spectrophotometer.

To do this, 250 µL of each preparation (except Blank PLGA nanoparticles) were lyophilized, in a total volume of 1 mL, at -80 °C for 12 hours. Lyophilized nanoparticles were then dissolved in 1 mL of acetonitrile to extract CUR into acetonitrile for the encapsulation efficiency calculation. Afterwards, the three CUR NPs preparations were vortexed and centrifuged at 3166x *g* for 10 minutes at 4° C. The supernatant (100 µL) was collected and plated in a 96 well-plate and the absorbance was measured at 450_{nm} in a microplate reader (Synergy™ Mx, BioTek Instruments Inc.) and analyzed with the Gen5™ software. A standard plot of CUR (ranging from 0.2 to 0.016 mg/ml) was prepared by dissolving CUR into acetonitrile and the absorbance was measured under the same conditions.

The % of encapsulation efficiency was calculated using the following formula:

$$Encapsulation\ Efficiency\ (\%) = \frac{Concentration\ of\ curcumin\ in\ the\ nanoparticles}{Initial\ concentration\ of\ curcumin} \times 100$$

3.5. Study of the *in vitro* cytotoxic effect of CUR and curcumin loaded PLGA nanoparticles in the Hs 578T cell line

The potential cytotoxic effect of CUR and CUR loaded PLGA nanoparticles was analyzed with the SRB colorimetric assay following the protocol described above (section 2.2) with minor modifications.

In this case, the Hs 578T cells were plated in 96-well plates at a density of 2×10^4 cells/mL and incubated at 37 °C for 24 hours to allow cell attachment. After this time, the T0 plate was fixed with TCA and five serial dilutions of CUR or curcumin loaded PLGA nanoparticles were prepared ranging from 40 to 1.25 µM.

Curcumin was freshly dissolved in DMSO before each assay, to avoid curcumin degradation, to a final concentration of 60 mM. Serial dilutions of CUR were prepared in medium, ranging 40 to 1.25 µM.

Blank PLGA nanoparticles were prepared under the same conditions of CUR loaded PLGA nanoparticles and were used as control. The nano-formulations solvent (DI water) and CUR solvent (DMSO) were also used as controls. Cells were incubated with the compounds and respective controls for 24 hours and then, the treatments were removed and 200 µL of medium (complete culture medium with 5% FBS) were added. Cells were maintained at 37 °C for further 72h (i.e. a total incubation time of 96 hours after the addition of the compounds).

After 96 hours of incubation, the T96 plate was fixed and SRB was added and washed with acetic acid as previously described. The absorbance was measured at 510_{nm} in a microplate reader and analyzed with the Gen5™ software. The GI_{50} values were then calculated, also as previously described. **Figure 10** is a schematic representation of the workflow.

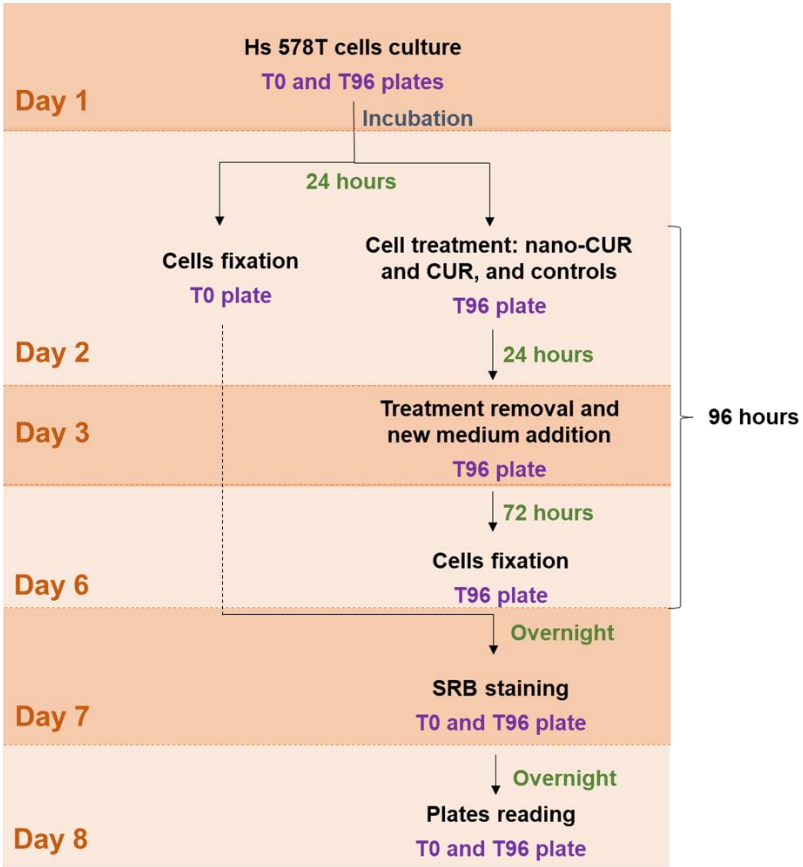

Figure 10. Description of the workflow of the SRB assay for the measurement of the cytotoxic effect of CUR or CUR-loaded PLGA nanoparticles.

4. Study of the *in-vitro* cytotoxic effect of CUR and CUR-loaded PLGA nanoparticles in sorted Hs 578T stem-like cells

The Hs 578T cell line was selected to characterize and isolate the stem-like cells.

Two specific markers were selected for Hs 578T breast cancer stem-like cells isolation: ALDH1 enzymatic activity and high expression of the cell surface marker CD44.

4.1. Characterization of ALDH$^+$ and CD44$^+$ expression on the Hs 578T cells using a BD FACSCanto™ flow cytometer

The ALDH1 activity was detected using the ALDEFLUOR™ kit (Stem Cell Technologies, Canada) according to manufacturer's protocol with minor modifications [96] in the Hs 578T cell line.

Cell concentration for the detection of ALDH1 activity was optimized for the Hs 578T cell lines. With that purpose, two cellular concentrations (2 x 10^5 cells/mL and 4 x 10^5 cells/mL) were tested for ALDH1 and CD44 characterization, using the FACSCanto™ flow Cytometer. For that, cells were washed twice with phosphate buffered saline (PBS) 1x (Sigma Aldrich) and detached with versene 1x (Gibco, UK). Detached cells were resuspended in fresh medium, centrifuged for 5 minutes at 288x *g* and counted using the Trypan Blue exclusion assay. Then, 2 x 10^5 cells/ml were resuspended and incubated in Aldefluor assay buffer containing 5 µL of the ALDH substrate, BODIPY-aminoacetaldehyde (BAAA), at 37°C for 45 min. The enzymatic activity of ALDH was blocked with 5 µL of the specific inhibitor DEAB, diethylaminobenzaldehyde. After incubation, cells were stained with 10 µL of allophycocyanin (APC)-conjugated anti-CD44 (1:10, BD Biosciences) and incubated on ice in the dark for 20 minutes. Finally, cells were washed and resuspended in fresh buffer with 1 µg/mL of the vital dye 7-actinoaminomycin-D, 7-AAD (Sigma Aldrich).

A sample stained for each single fluorescent marker used in the experiment [BAAA, (APC)-conjugated anti-CD44 (1:10) and 7-AAD (1 µg/mL)] and an unstained sample were prepared for both cell lines to adjust photomultiplier tube (PMT) voltages and set up compensations.

Data were analysed using BD FACSDiva™ software: the gate for ALDH+ was drawn relative to baseline fluorescence, which was determined by DEAB-treated cells. The

percentages of Hs 578T stem-like cells ($ALDH^+/CD44^{high)}$ and Hs 578T non-stem like cells ($ALDH^-/CD44^{low}$) were determined.

4.2. Isolation of stem-like ($ALDH^+/CD44^{high}$) and non-stem ($ALDH^-/CD44^{low}$) populations from the Hs 578T cell line using a BD FACS Aria II flow cytometer

The isolation of Hs 578T stem-like cells ($ALDH^+/CD44^{high}$) and non-stem like cells ($ALDH^-/CD44^{low}$) was performed following the above described protocol (section 4.1.)

After that, both Hs 578T populations were sorted using the BD FACSAria™ II flow cytometer (BD Biosciences). $ALDH^+/CD44^{high}$ and $ALDH^-/CD44^{low}$ were collected to two 15 mL tubes in RPMI-1640 supplemented with 20% FBS and 1% antibiotic/antimycotic for the following assays.

4.3. Analyzing the recovery of the sorted Hs 578T stem-like cells

Hs 578T sorted populations ($ALDH^+/CD44^{high}$ and $ALDH^-/CD44^{low}$) were plated in 96-well plates (T0 and T96), according to the above described protocol (Section 3.5.). After cell sorting, two time points (24 and 48 hours) were tested for analyzing the cell recovering.

After 24 or 48 hours of incubation, the T0 plates were fixed and the SRB assay was performed, as previously described (section 2.2.). After 96 hours of incubation, the same procedure was performed for the T96 plates.

Results and discussion

I. Cell growth inhibitory activity of *Eucalyptus globulus L.* and *Melissa officinalis L.* extracts in the Hs 578T and the BT-20 cell lines

For the cytotoxicity experiments, it is important to guarantee an exponential cell growth for the entire period of the assay. Consequently, cells should not be allowed to reach 100% confluency at the end of the experiment. This confluency may lead to exhaustion of the growth medium, cell cycle arrest and apoptosis, which can cause a significant change in the calculation of GI_{50} values [97, 98].

Since the optimal number of cells to seed is dependent of the doubling time of each cell line, the optimal cell density to be plated in a 96 well-plate, for 48h long assays, was determined for the Hs 578T and BT-20 cell lines.

Different concentrations of cells were seeded in 96 well-plates (ranging from 1 x 10^4 to 1 x 10^5 cells/mL for the Hs 578T cell line and from 2 x 10^4 to 2 x 10^5 cells/mL for BT-20 cell line) and the cell incubation conditions used in the SRB assay were reproduced. Therefore, cells were analyzed 48h latter, under an inverted microscope. The results are shown in **Figure 11**.

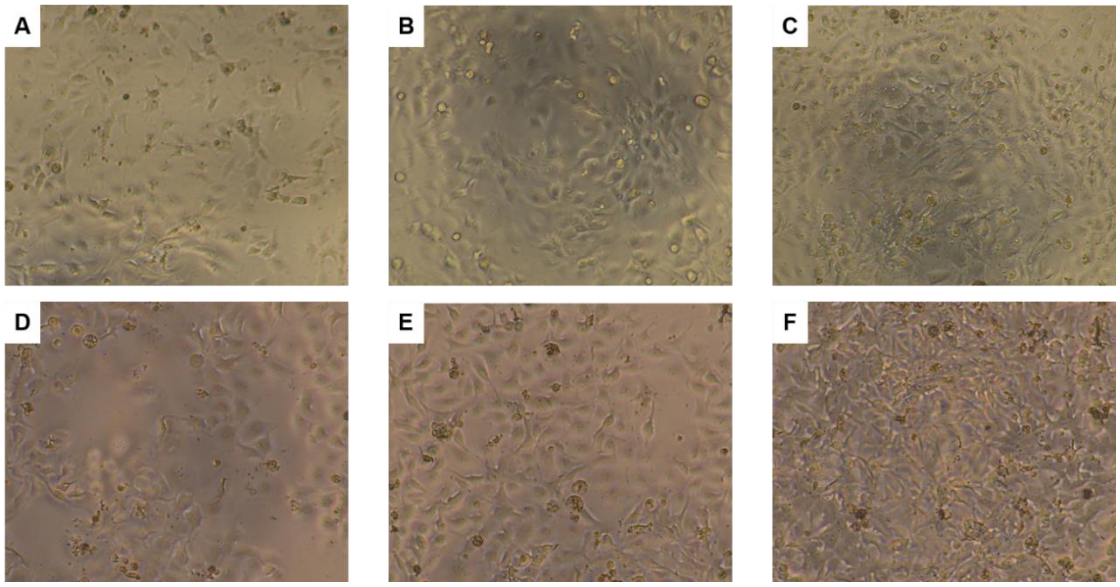

Figure 11. Representative images of Hs 578T and BT-20 cell lines at the end of the assay. *(**A**) Hs 578T plated as 2 x 10^4 cells/mL; (**B**) Hs 578T plated as 4 x 10^4 cells/mL; (**C**) Hs 578T plated as 5 x 10^4 cells/mL; (**D**) BT-20 plated as 8 x 10^4 cells/mL; (**E**) BT-20 plated as 10 x 10^4 cells/mL; (**F**) BT-20 plated as 20 x 10^4 cells/mL. (Magnification, x100).*

At the end of the experiment, cells should have reached approximately 70-80% of confluence [98]. This percentage was reached for 4 x 10^4 cells/mL for Hs 578T cells and for 10 x 10^4 cells/mL for the BT-20 cells, at the endpoint of 48 hours [See **Figure 11 (B) and**

(E)]. Therefore, these cellular concentrations were later used for performing the SRB assay in 96 well-plates for 48h. As shown in **Figure 11**, lower or higher concentrations caused an insufficient (**Figure 11, A & D**) or excessive (**Figure 11, C & F**) confluence at the end of the experiment.

The growth inhibitory effect of the natural extracts *Eucalyptus globulus* and *Melissa officinalis* was then tested in these two cell lines, using the SRB colorimetric assay. This technique relies on the ability of SRB to bind (electrostatically and pH dependently) to basic amino acid residues of the protein components of fixed cells. As the binding of SRB is stoichiometric, this assay allows to indirectly infer on cell growth, considering that the amount of staining is directly proportional to the number of cells [95, 97, 99]. The GI_{50} of each extract was determined and the results are summarized in **Table 3**.

Table 3. GI_{50} concentrations of Eucalyptus extracts in the breast cancer cell lines Hs 578T and BT-20 and of Melissa officinalis in the Hs 578T cell line.

	GI_{50} (µg/mL)	
	Hs 578T	**BT-20**
***Eucalyptus* Infusion**	30.4 ± 3.65	136.6 ± 8.5
***Eucalyptus* decoction**	28.4 ± 4.10	114.4 ± 4.8
Melissa officinalis	24.3 ± 4.24	n.d.

The GI_{50} concentrations were determined with the SRB assay and are represented as the mean ± SE. Doxorubicin was used as positive control, and its GI_{50} were the following: 161.5 ± 30.3 nM for the Hs 578T cells and 45.4 ± 9.3 nM for the BT-20 cells. n.d.= not determined. Representative data from n=4 independent experiments for the Hs 578T cell line and from n=3 independent experiments for the BT-20 cell lines

Cells were incubated with five serial dilutions (1:2) of each extract ranging from 200 to 12.5 µg/mL for 48h. Moreover, the effect of the compound's solvent (distilled water) was also analyzed. Therefore, both cell lines were treated with the maximum volume of water used for preparing the higher concentration of each extract. No effect of the distillated water was detected in any of the experiments (data not shown).

Doxorubicin, a potent chemotherapeutic drug approved to treat BC [100], was used as positive control. Both cell lines were incubated with serial 1:2 dilutions of Doxorubicin

ranging from 1250 to 78.1 nM for the Hs 578T cells and from 150 to 9.4 nM for the BT-20 cells. It was verified that Doxorubicin has growth inhibitory effect in both cell lines, presenting a GI_{50} concentration of 161.5 ± 30.3 nM (for Hs 578Tcells) and 45.4 ± 9.3 nM (for BT-20 cells). These values are relatively similar to the ones found in the literature (IC_{50} concentration of 9.2μM [101] for Hs 578T cell line and IC_{50} concentration of 34.7 nM [102] for BT-20 cell line), taking in consideration that we calculated GI_{50} and the authors of these publications calculated IC_{50} and also taking into consideration the fact that they performed the assay for 24h (for Hs 578T cell line).

The obtained results show that the cytotoxic effects of the three extracts are higher in the Hs 578T cells than in the BT-20 cells (**Table 3**). These differences suggest that these extracts might have a specific effect in some cells. Results also indicate that both extracts exhibit similar growth inhibitory effect in each cell line, presenting GI_{50} concentrations ranging from 24.3 to 30.4 μg/mL in the Hs 578T cell line and ranging from 114.4 to 136.6 μg/mL in the BT-20 cell line.

Additionally, in Hs 578T cells it is possible to observe that higher concentrations of the three extracts (>50 μg/mL) reduced the percentage of control cell growth to values lower than the initial number of cells **(Figure 12)**, suggesting that these extracts induce some degree of cell death in this cell line. This effect was not observed in the BT-20 cells, in which only the *Eucalyptus* decoction extract exerted this effect at a concentration of 200 μg/mL (**Figure 12**). Therefore, there is no evidence that the tested extracts induce cell death in the BT-20 cells, bellow the maximum concentration tested of 200 μg/mL.

Indeed, cytotoxic studies with different *Eucalyptus* species have been undertaken, revealing positive effects against some cancer cell lines such as breast, colon, lung, liver and others [69, 103]. In particular, Inês et al. [103] showed that *Eucalyptus globulus* has antioxidant activity against the human TNBC cell line MDA-MB-231, with an IC_{50} concentration of 91.9 ± 9.04 μg/mL (the IC_{50} value represents the concentration that inhibits 50% of cell viability). The authors of this study calculated the IC_{50} (instead of using our approach of calculating the GI_{50}), which could justify the apparent difference between the two studies; furthermore, differences between our study and the one by Inês et al. [103] may also depend on the part of the plant from which the extracts were sourced and on the extraction methods used.

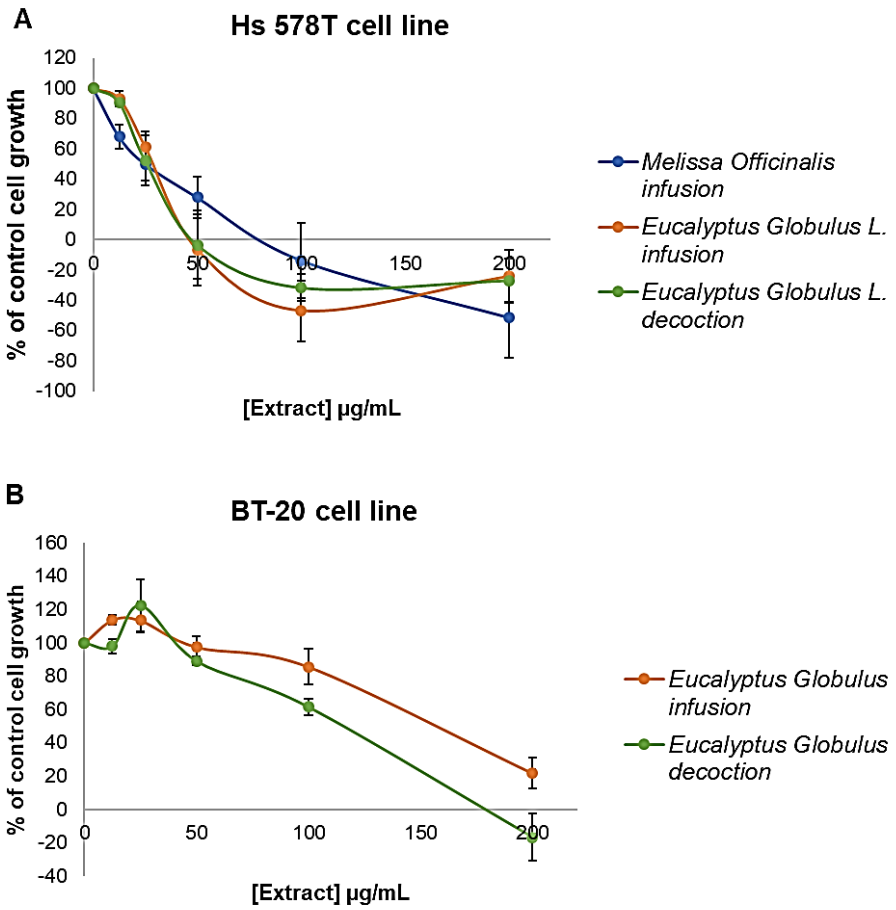

Figure 12. Dose-response curves of the natural extracts in the Hs 578T (A) and BT-20 (B) cells. *The results were determined with the SRB assay and are presented as percentage (%) of cell growth when compared to cells treated with the solvent (water) and the no growth control (T0 plate). Representative data from n=4 independent experiments for the Hs 578T cell line and from n=3 independent experiments for the BT-20 cell lines*

In addition, Saraydin et al. [104] investigated the antitumor activity of *Melissa Officinalis* in different breast cancer cell lines, including the TNBC MDA-MB-231 and MDA-MB-468 cell lines. These authors also verified that this extract is potent in the two TNBC cell lines studied, presenting IC_{50} concentrations of 19 ± 1.8 µg/mL in MDA-MB-231 and 17 ± 1.4 µg/mL in MDA-MB-468 cells.

It is known that patients with TNBC have a poor clinical outcome. This subtype of BC is characterized by the shortest survival, high proliferation levels, development of recurrence and distant metastasis [30].Therefore, the discovery of new cytotoxic agents for the development of more effective treatments for these patients is crucial. Taken together, the

obtained results indicate that these extracts have dose-dependent cytotoxic effects in both the TNBC cell lines used in this study, presenting a more potent effect in the Hs 578T cells.

II. Developing of curcumin loaded PLGA [poly(lactic-co-glycolic acid)] nanoparticles

Curcumin (CUR), a bioactive compound isolated from Turmeric, has demonstrated antitumor activity against several tumors, including BC [105]. CUR is considered a promise and potent anticancer agent since it can target multiple pathways important in cancer [85] and can eliminate breast CSCs [106]. However, the reduced solubility and low bioavailability of CUR limit its use in the clinic [81]. Therefore, effective CUR encapsulated PLGA nanoparticles were developed via nanoprecipitation technique and stabilized with Poloxamer 407.

The selection of the right polymer composition, stabilizer, solvent and technique is fundamental to achieve an efficient drug encapsulation [107].

The nano-precipitation method was selected to prepare the nanoparticles (NPs), since this technique is simple, fast and easy to duplicate in practice and does not require a sonication step [108, 109].

PLGA was used due to its biocompatibility and biodegradability rate. It allows protection of the drug from degradation and sustained drug delivery [89].

With the aim of optimizing the amount of CUR incorporated into PLGA nanoparticles, three different initial concentrations of CUR were tested (1mg, 0.5mg and 0.1mg, **Figure 13**).

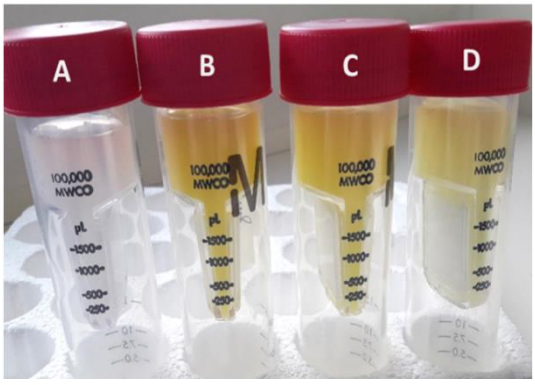

Figure 13. PLGA nano-formulations in Amicon Filters®. *(A) Blank NPs; (B) 1 mg/mL CUR NPs; (C) 0.5 mg/mL CUR NPs; (D) 0.1 mg/mL CUR NPs*

The physico-chemical characteristics of the three different nano-CUR and Blank NPs [e.g. particle size, polydispersity index (PDI), zeta potential and percentage of curcumin encapsulation] are summarized in **Table 4**. The polydispersity index (PDI) indicates the range of particles distribution in the formulation and results should range from 0 to 1, where

zero indicates a monodispersed and homogeneous formulation. In the case of PLGA nanoparticles, values up to 0.3 are considered a good monodisperse system [107]. The zeta potential is an indicator for the nanoparticles surface charge [110].

Table 4. Physico-chemical characterization of PLGA-CUR nano-formulations.

	Size (d.nm)	PDI	Zeta Potential (mV)		EE (%)
Blank NPs	267 ± 4.0	0.3 ± 0.02	-27.6	± 1.07	n.d.
CUR NPs 1 mg	312 ± 4.44	0.3 ± 0.04	-29.3	± 2.00	50 ± 5
CUR NPs 0.5 mg	241 ± 9.2	0.1 ± 0.01	-26.2	± 0.59	63 ± 3
CUR NPs 0.1 mg	290 ± 14.6	0.2 ± 0.004	-28.6	± 2.20	36 ± 4

Size, Polydispersity Index (PDI) and Zeta Potential were measured using the Zetasizer and are the mean ± SE. The % of encapsulation efficiency (EE) was measured by a direct method and the presented values are the mean ± SE. **CUR NPS 0.1 mg, 0.5 mg and 1 mg =** CUR NPs prepared with an initial CUR concentration of 0.1 mg, 0.5 mg and 1 mg respectively; **n.d.=** not determined. Representative data from n=5 independent experiments (for Blank NPs and CUR NPs 0.5 mg) or n=3 independent experiments (for CUR NPs 0.1 mg and 1 mg)

The particle size, zeta potential and PDI were measured with a Zetasizer. Particle size can affect the biodistribution, physical stability, cellular uptake and drug release [111]. Usually, the smaller the particle size, the better the performance [112]. Results show that the NPs prepared with an initial CUR concentration of 1 mg and 0.1 mg exhibit the larger particle size (312 ± 4.4_{nm} and 290 ± 14.6_{nm}, respectively) and a more heterogeneous formulation (PDI = 0.3 ± 0.04 and 0.2 ± 0.004, respectively) while particles prepared with an initial CUR concentration of 0.5 mg exhibit smaller particle size (241 ± 9.2_{nm}) and a homogeneous formulation (PDI = 0.1 ± 0.01). According to the literature, these sizes were expected to be lower than the obtained ones. Indeed, other authors, also using the nanoprecipitation technique, prepared CUR NPs with mean sizes around 100 nm [113]. However, in our study, these values were not achieved. Nevertheless, Yallapu *et al*. [107] developed six different CUR NPs differing in the stabilizer's concentrations used. They verified that the particles size ranged from 76.2 ± 5.36 nm to 560.4 ± 10.95 nm, corresponding to the NPs prepared with the highest and lowest concentrations of the stabilizer poly(vinyl alcohol) (PVA), respectively. Since in our study the stabilizer used was the Poloxamer 407, these findings suggest both the choice of the stabilizer to be used and its concentration may influence the particle size, and that this may be a cause for differences in the attained data.

Results also show that there is an increase in the particle size of the NPs prepared with an initial CUR concentration of 1 mg and 0.1 mg (312 ± 4.44 $_{nm}$ and 290 ± 14.6 $_{nm,}$ respectively) compared to the unloaded NPs (Blank NPs) (267 ± 4.0$_{nm}$). This effect is possibly due to the fact that the drug causes an expansion of the polymeric matrix, leading to an increase in the particle size [114]. Nonetheless, the same is not observed with the NPs prepared with an initial CUR concentration of 0.5 mg (241 ± 9.2$_{nm}$), which have a smaller particle size than the Blank NPs.

Zeta Potential values are negative as expected, due to PLGA carboxylic end-groups, ranging from -26 to -29 mV. Zeta Potential values slightly increases from -27.6 ± 1.07 mV in Blank NPs to -26.2 ± 0.59 mV in NPs prepared with an initial CUR concentration of 0.5 mg. This increase could be explained by CUR adsorption on the PLGA NPs surface, since the drug adsorbed on PLGA NPs surface exerts a masking effect of the superficial carboxylic groups, reducing the effective NP charge [114]. The same is not observed in the NPs prepared with an initial CUR concentration of 1 mg and 0.1 mg, where there is a slightly decrease from -26.2 ± 0.59 mV in Blank NPs to -29.3 ± 2.00 mV and -28.6 ± 2.20 mV in NPs prepared with an initial CUR concentration of 1 mg and 0.1 mg respectively.

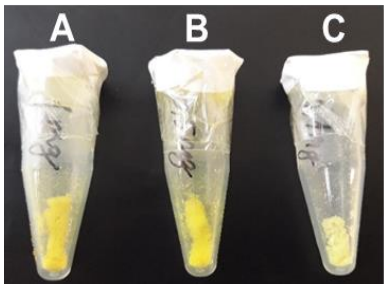

Figure 14. Liphilized CUR nanoformulations. *(A) 1 mg/mL CUR NPs; (B) 0.5 mg/mL CUR NPs; (C) 0.1 mg/mL CUR NPs.*

The percentage of encapsulation efficiency was measured by a direct method. The loaded NPs formulations were lyophilized (**Figure 14**) and then resuspended in acetonitrile. The absorbance was measured at 450$_{nm}$. A standard curve of CUR concentration versus Absorbance at 450nm was prepared and used for determination of CUR concentrations (**Figure 15**). The obtained results for the encapsulation efficiency (EE) of both formulations are expressed in % of encapsulation (**Table 4)**.

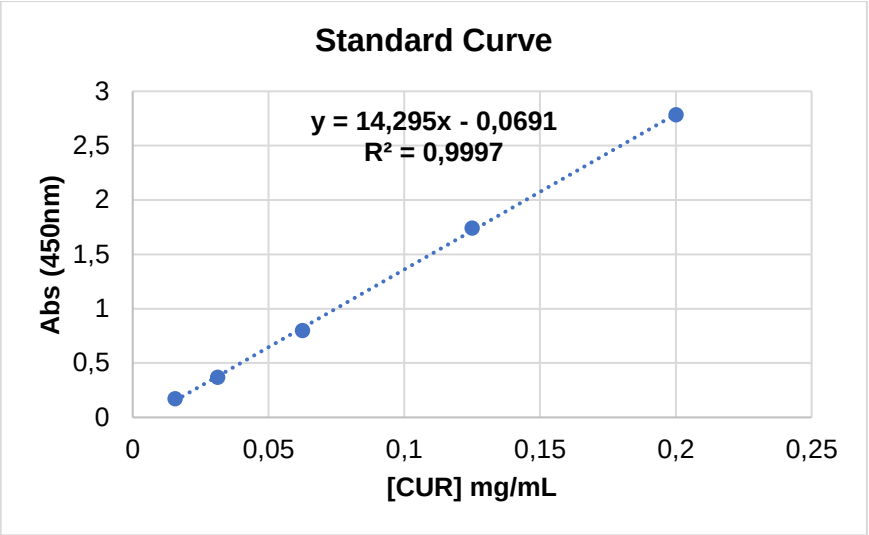

Figure 15. Standard curve of CUR concentration versus Absorbance at 450nm.

PLGA-based NPs commonly present high encapsulation efficiency, that can range from 6-90%. The mean of encapsulation efficiency generally is around 60-70% for different drugs (e.g. xanthones and estradiol) [93]. The obtained results for EE are in line with these values, ranging from 36% to 63% as is shown in **Table 4**. The % of encapsulation of CUR in the three different formulations indicates a clear variation. The higher percentage of encapsulation efficiency (63 ± 3%) was achieved in the particles prepared with an initial CUR concentration of 0.5 mg. The other two formulations have smaller % of encapsulation (50 ± 5% and 36 ± 4% for particles prepared with an initial CUR concentration of 1 mg and 0.1 mg respectively). The lower % of encapsulation may be due to a minimal swelling capacity of the PLGA macromolecular chains to entrap curcumin in aqueous media [115].

Regarding these results, the CUR NPs prepared with an initial CUR concentration of 0.5 mg were selected for the *in vitro* cytotoxic experiments, since they presented the smaller particle size, the highest EE and a homogeneous formulation which may improve its cytotoxic effects in cells.

III. *In vitro* cytotoxic effect of CUR and CUR-loaded PLGA nanoparticles in the Hs 578T cell line

The *in vitro* cytotoxic effect of CUR and the selected CUR-loaded NPs was assessed with the SRB colorimetric assay in Hs 578T cell line.

Cells were initially treated for 48 hours with five serial dilutions of CUR or CUR-loaded PLGA NPs ranging from 40 to 1.25 μM. However, it was not possible to determine the GI_{50} concentration of CUR NPs with this layout, as shown in **Table 5**. This could be due to the properties of the NPs that provide a sustained release of CUR and avoid its rapid deliver.

Table 5. ***GI_{50} concentrations of the CUR NPs in the Hs 578T cells treated for 48 hours.***

	GI_{50}(μM)
	Hs 578T
CUR	12.61
CUR NPs	> 40
Blank NPs	> 40

The GI_{50} concentrations were determined with the SRB assay and are representative of one independent experiment only.

It is important to note that the curcumin entrapped in the PLGA NPs is not in direct contact with the cells. The drug release from the PLGA copolymer is a complex process which involves the degradation of the polymer [91]. Therefore, more time is needed to allow the release of CUR.

Consequently, in the following experiments the incubation time was increased to 96 hours. In this case, 24 hours after cells seeding (2 x 10^4 cells/mL), CUR or CUR-loaded NPs were added to the cells as previous described and Blank NPs were used as control. After 24 hours of incubation, the compounds were removed, and fresh medium was added to the cells. Cells were incubated at 37° C for further 72h (a total time of 96 hours). The obtained results are presented in **Table 6**.

Results show that, as expected, Blank NPs have no effect on cell viability indicating no toxicity of the empty NPs in this cell line. The same is observed with distilled water (data not shown), which means that this solvent has no cytotoxic effect on these cells. Both CUR and CUR-loaded NPs presented dose dependent cell growth inhibition effects.

Table 6. **GI_{50} concentrations of the CUR-loaded NPs in the Hs 578T cell line treated for 96 hours.**

	GI_{50}(μM)
	Hs578T
CUR	7.1 ± 0.3
CUR NPs	23.3 ± 3.4
Blank NPs	> 40

The GI_{50} concentrations were determined with the SRB assay and are the mean ± SE. Representative data from n=3 independent experiments

CUR exhibits the most potent cell growth inhibitory activity (GI_{50} 7.1 ± 0.3 μM) when compared with CUR-loaded NPs (GI_{50} 23.3 ± 3.4 μM). Inversely, Yallapu *et al*. [107] developed a CUR-loaded NPs formulation which presented a higher anti-proliferative effect when compared with free CUR in the MDA-MB-231 BC cell line, with IC_{50} concentrations of 9.1 μM and 16.4 μM respectively. However, these authors developed a nanoparticle formulation using a different stabilizer, PVA, which may justify the obtained results. The same observation was made by Anand et al. [113] in the same cell line (MDA-MB-231), using a nanoparticle formulation based on PLGA and the stabilizer polyethylene glycol (PEG)-5000.

It is also possible to observe (**Figure 16**) that concentrations of CUR >20 μg/mL reduced the cell number to values lower than the initial number of cells, indicating that CUR induced some degree of cell death on the Hs 578T cells. The same was not observed for the CUR-loaded NPs, maybe because of the sustained and controlled release of CUR promoted by PLGA NPs. A similar observation was also verified by Yallapu *et al*. [107] for CUR NPs, but not for free CUR.

CUR exhibit the most potent cell growth inhibitory activity (GI_{50} 7.1 ± 0.3 μM) when compared with CUR-loaded NPs (23.3 ± 3.4 μM). However, CUR has poor solubility in water, which limits its possible use in the clinic. Due to its insolubility in water, CUR was dissolved in DMSO, which would not be compatible with a therapeutical application [116]. Even though it is believed that nanotechnology may improve the solubility and stability of curcumin, which may reduce its bioavailability problems, the NPs formulations described in the present work need to be further improved. Further improvement of the here described NPs may consist in testing different stabilizers, and in different concentrations.

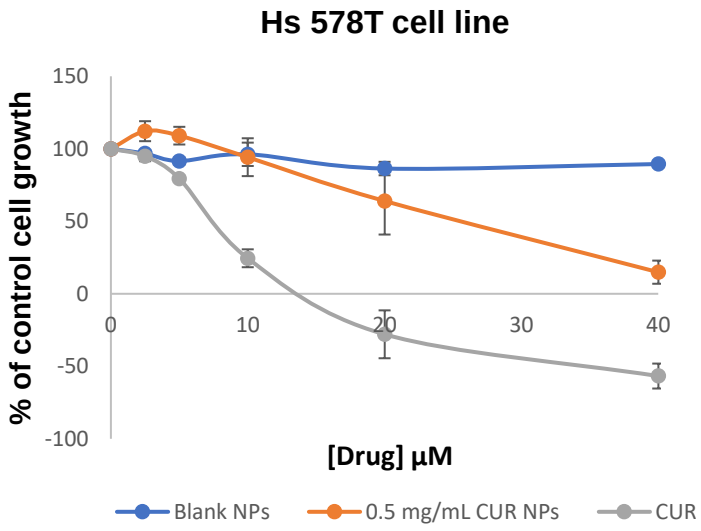

***Figure 16. Dose-response curves of CUR and CUR-loaded NPs in the Hs 578T cell line**. The results were determined with the SRB assay. Five serial dilutions of the compound or formulations were tested for 96hours, ranging from 40 to 2.5 µM. Results are presented as % of cell growth when compared to cells treated with the solvent (water for the nano-formulations and DMSO for CUR) and to the no growth control (T0 plate). Representative data from n=3 independent experiments*

IV. In-vitro cytotoxic effect of CUR and curcumin loaded PLGA nanoparticles in Hs 578T stem-like cells

CSCs represent a small population of cells within a tumor with self-renewal and differentiation capacity and high proliferative potential. These cells are responsible for tumor growth and are frequently associated with tumor metastasis, heterogeneity and cancer treatment failure [40]. Since they are resistant to conventional therapies, CSCs identification is extremely valuable for the development of more effective treatments [38]. Recent studies have shown that CUR has a great potential to inhibit CSCs in different cancer types [85].

TNBC is considered the most heterogeneous group of breast cancer. Patients with this type of breast cancer have poor clinical outcome with prevalence of recurrence and distant metastasis [29]. The triple negative Claudin-Low subgroup is believed to be enriched with cancer stem-cell-like features [36], therefore, the Hs 578T cell line (representative of Claudin-Low cells) was selected to attempt to characterize and isolate stem-like cells.

The most frequent used method to identify CSCs is based on the expression of specific markers. However, these markers are distinct in different tumor types and organs. In case of breast CSCs, the most commonly used markers are the CD44 and CD24 expression and

the ALDH1 activity [51, 60, 117]. Therefore, in this work, two specific markers were selected for Hs 578T breast cancer stem cells isolation: ALDH1 enzymatic activity and high expression of the cell surface marker CD44.

The Hs 578T stem-like cells were isolated, based on the above-mentioned markers, using the ALDEFLUOR™ assay kit, for the detection of ALDH1 activity, in combination with the allophycocyanin (APC)-conjugated anti-CD44 antibody. The expression levels of both markers were determined by flow cytometry.

i. Evaluation of ALDH1 activity in the MKN-45 and Hs 578T cell lines

The ALDH1 activity was measured using the ALDEFLUOR™ kit. This assay was initially developed for the detection of hematopoietic stem cells. Therefore, the cell concentration to be used for the detection of ALDH1 activity must be optimized.

The MKN-45 cell line was used as a positive control for ALDH1 activity, since it was previously demonstrated that this cell line contained a high percentage of cells with ALDH1 activity [118]. To optimize the cell concentration to be used in this assay, two different concentrations of MKN-45 (2×10^5 cells/mL and 1×10^6 cells/mL) and of Hs 578T (2×10^5 cells/mL and 4×10^5 cells/mL) were tested. The ALDH1 activity was detected using a FACSCanto™ flow Cytometer.

Cells were incubated with the ALDH substrate, BAAA. In cells with ALDH1 activity, BAAA is catalyzed into its fluorescent product, BODIPY aminoacetate (BAA), thus, positive cells for ALDH1 will retain the product and emit fluorescence.

The positive and negative populations for ALDH1 were determined by using an inhibitor of ALDH1 activity, the DEAB.

FACS analysis revealed that both concentrations tested exhibited a high percentage of MKN-45 cells with ALDH1 activity (**Figure 17**). Interestingly, it was detected that the lowest cell concentration tested (2×10^5 cells/mL of buffer) contained a high percentage of cells with ALDH1 activity (34.7%) (**Figure 17A**) when compared with the highest cell concentration analyzed (1×10^6 cells/mL of buffer) with a percentage of 22.9% (**Figure 17B**). These results suggest that the 2×10^5 cells/mL of buffer is a good cell concentration for the detection of ALDH1 activity in MKN-45 cells. In addition, these percentages are in line with other studies [118, 119].

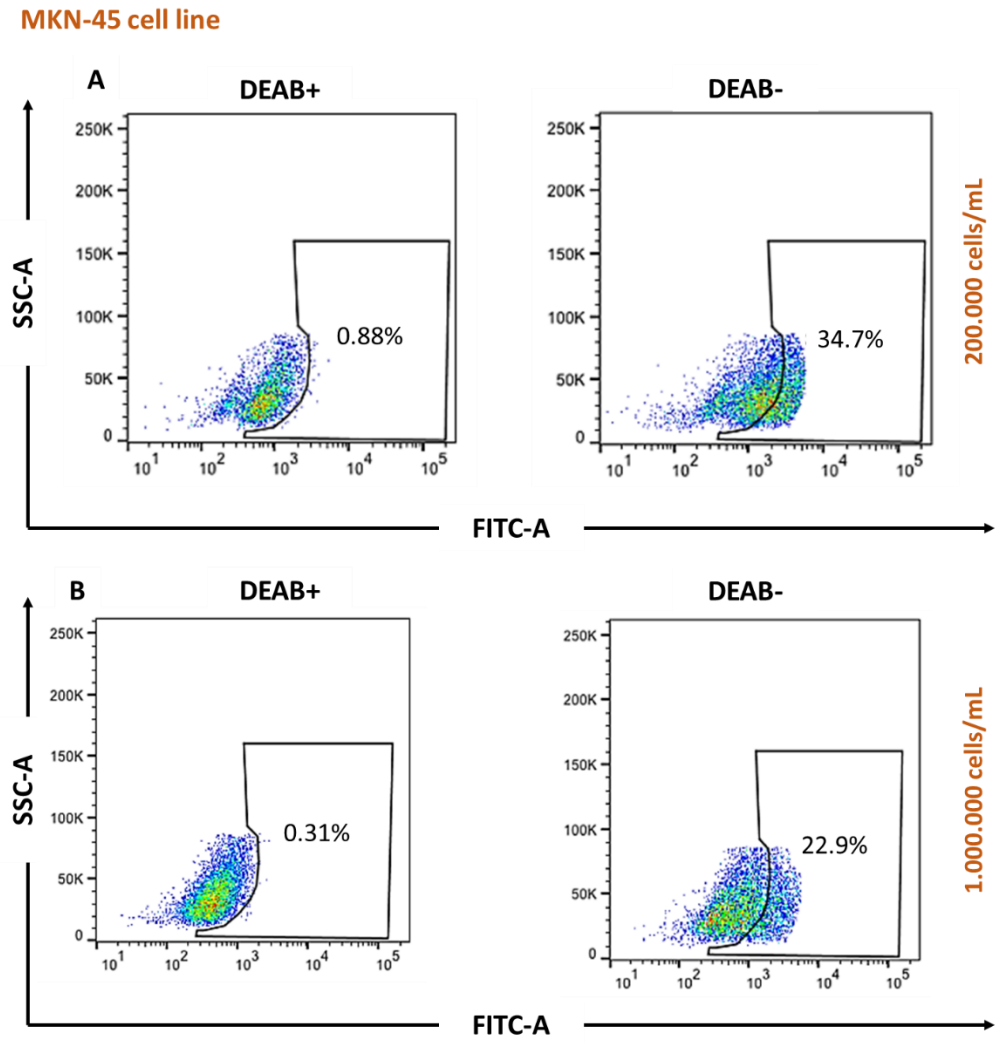

Figure 17. Detection of ALDH activity in the MKN-45 cell line. *DEAB was used as ALDH inhibitor. The gated cells were defined as ALDH⁺ cells.* ***(A)*** *Percentage of MKN-45 ALDH+ cells at a concentration of 2 x 10^5 cells/mL of buffer;* ***(B)*** *Percentage of MKN-45 ALDH+ cells at a concentration of 1 x 10^6 cells/mL of buffer. Data from one independent experiment.*

However, in the Hs 578T cell line (**Figure 18**), both concentrations tested contained similar % of cells with ALDH1 activity (1.8% and 2.5% for 2 x 10^5 and 4 x 10^5 cells/mL of buffer respectively). These low % are not corroborated by other studies in which a higher % of cells with ALDH1 activity was described for this cell line [120]. However, during this experiment, Hs 578T cells have only reached approximately 40-60% of confluence, which might have influenced the results. Consequently, these results are not conclusive.

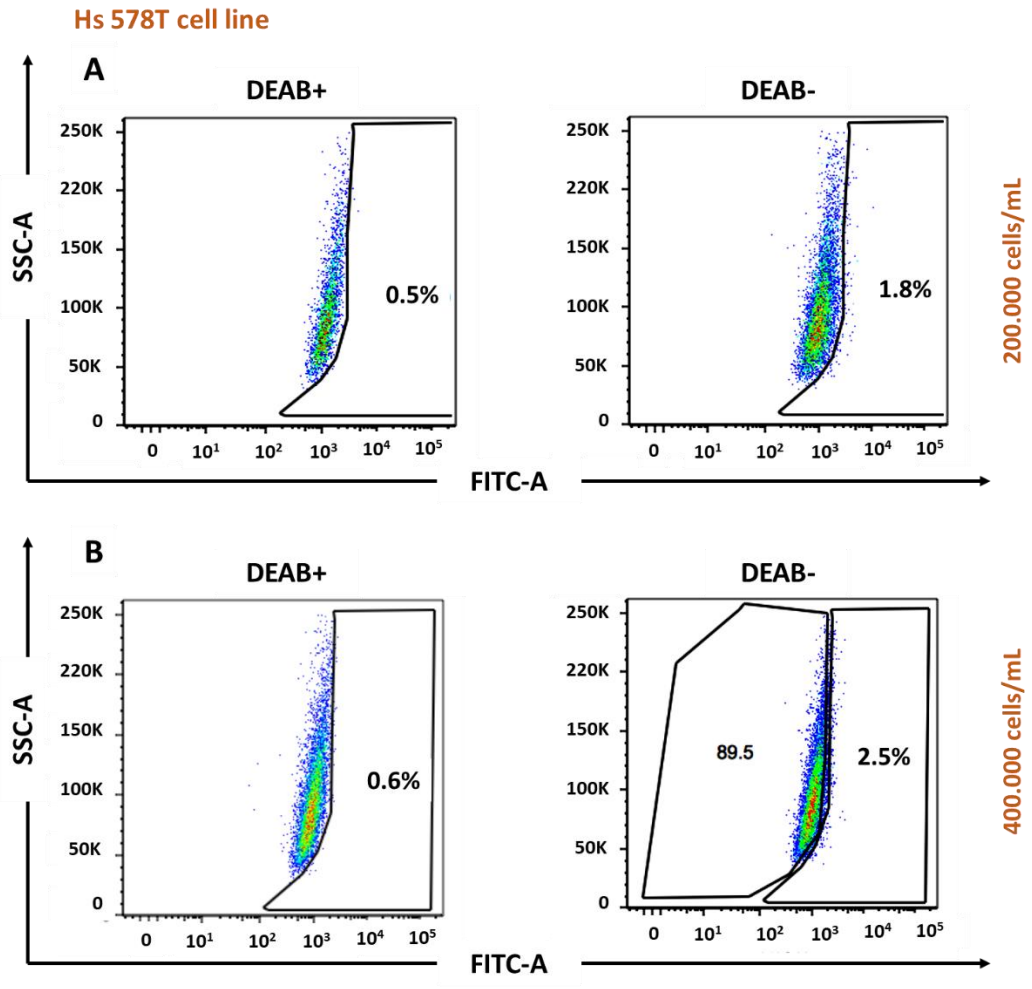

Figure 18. Detection of ALDH activity in the Hs 578T cell line. *DEAB was used as ALDH inhibitor. The gated cells were defined as ALDH⁺ cells.* ***(A)*** *Percentage of Hs 578T ALDH⁺ cells at a concentration of 2 x 10^5 cells/mL of buffer;* ***(B)*** *Percentage of Hs 578T ALDH⁺ cells at a concentration of 4 x 10^5 cells/mL of buffer. Data from one independent experiment.*

Given these very low numbers of obtained putative CSCs, the ALDEFLUOR™ assay was repeated once more in both cell lines. Since the previously obtained % of cells with ALDH1 activity in the Hs 578T cell line was similar when using both concentrations of cells, only 2 x 10^5 cells/mL of buffer were now used.

FASCS analysis revealed that the MKN-45 cell line (**Figure 19A**) maintained a % of ALDH⁺ cells (26.1%) similar to the one previously obtained. In addition, a higher % of ALDH⁺ cells was now observed (13.6%) in the Hs 578T cells (**Figure 19B**). Given the % of ALDH⁺ cells found in other studies with this cell line [120], this result was in agreement with the literature.

As the results were in line with the % of putative CSCs found in the literature and since the results for the MKN-45 cell line had been shown to be reproducible (twice), it was

concluded that the cell concentration of 2 x 10^5 cells/mL of buffer was good for the detection of ALDH1 activity in both cell lines.

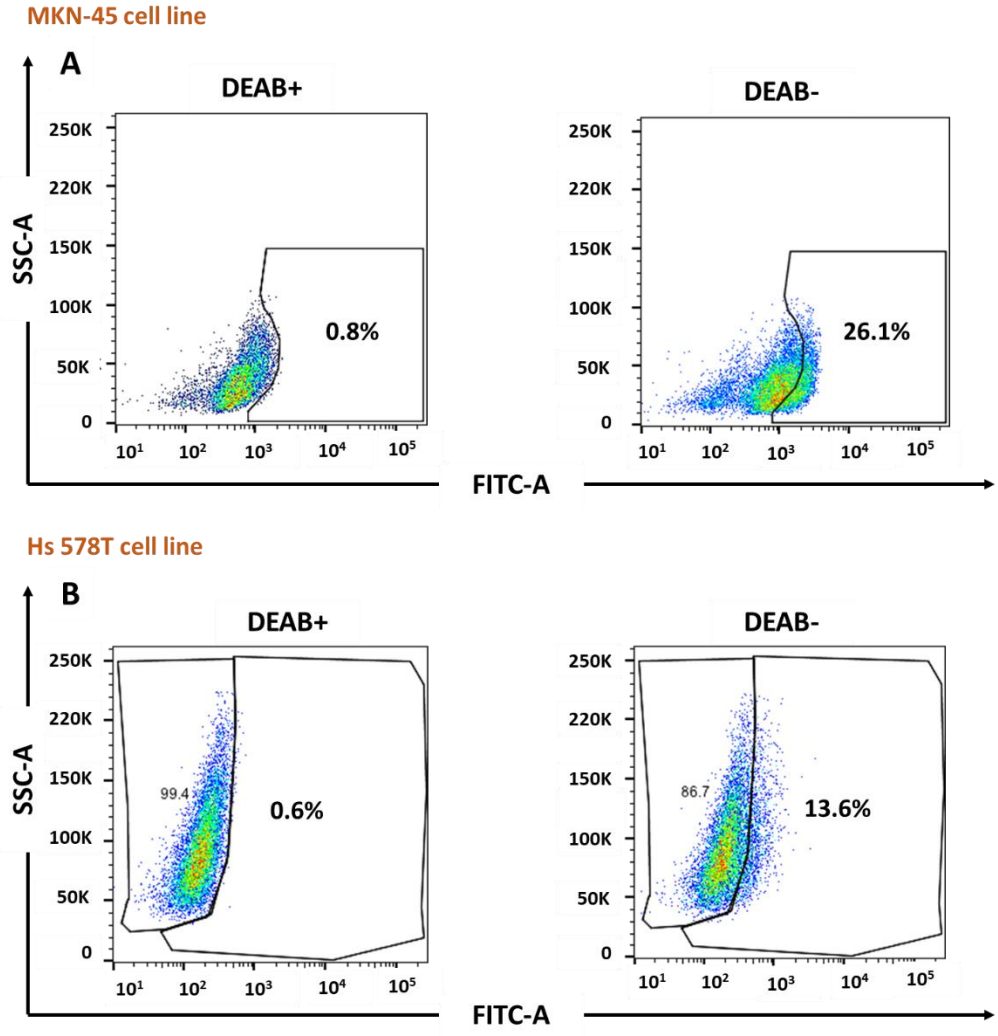

Figure 19. Detection of ALDH activity in the MKN-45 and Hs 578T cell lines. *DEAB was used as ALDH inhibitor. The gated cells were defined as ALDH⁺ cells.* ***(A)*** *Percentage of MKN-45 ALDH⁺ cells at a concentration of 2 x 10^5 cells/mL of buffer;* ***(B)*** *Percentage of Hs 578T ALDH⁺ cells at a concentration of 2 x 10^5 cells/mL of buffer. Data from one independent experiment.*

ii. Hs 578T cell line: Characterization of ALDH activity and CD44 expression using a BD FACSCanto™ flow cytometer

After defining the concentrations to be used for each line, the percentage of ALDH⁺ and CD44⁺ cells in the Hs 578T cell line was analyzed, using a FACSCanto™ flow Cytometer.

The ALDEFLUOR™ assay was performed in the Hs 578T cell line (2 x 10^5 cells/mL of buffer) in combination with labelling for CD44 with an allophycocyanin (APC)-conjugated anti-CD44 antibody.

Therefore, analysis of CD44 staining and detection of ALDH1 activity were performed by flow cytometry and the obtained data was analyzed using the BD FACSDiva v8.0.1 software. First, each single fluorescent marker was used to adjust the photomultiplier tube (PMT) voltages and set up compensations.

Data were organized through dot plots and each dot/point represents an individual cell. The percentage of $CD44^+$ cells and $ALDH^+$ cells was determined.

As shown in **Figure 20**, the majority of Hs578T cells were positive for CD44 (99.8 %). High levels of CD44 (>80%) was previously described by other authors [120, 121]. The fact that this cell line has such a high % of cells positive for CD44 expression suggests that CD44 may not be a good stem cell marker for this cell line (since the % of stem cells should be much lower). A possible explanation is that the CD44 antibody could not be labeling specifically.

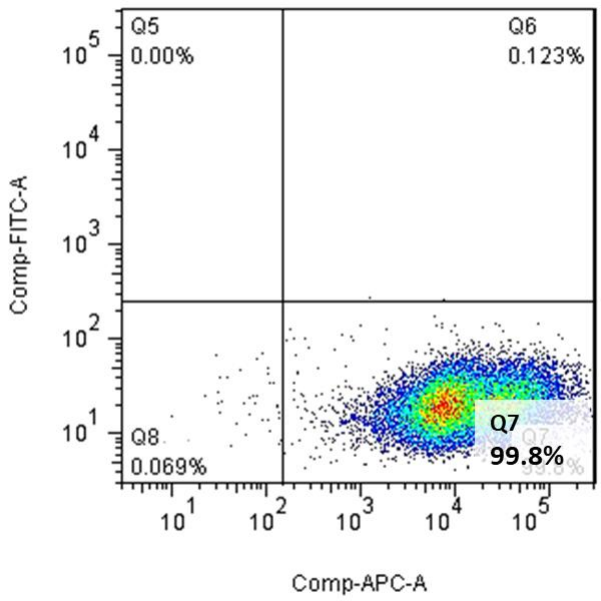

Figure 20. Expression of CD44 in the Hs 578T cell line. *Cells were stained with single APC-conjugated anti-CD44. Quadrants were set using appropriate FITC single fluorescent marker. The lower right quadrant represents $CD44^+$ cells. Data from one independent experiment.*

When testing this cell line for ALDH activity it was verified, by comparing with DEAB treated control group, that the $ALDH^+$ population was detected in 21.1% of the Hs 578T cells (**Figure 21**). This % was in agreement with the relatively low percentages of CSCs previously found in other studies, in this cell line [120].

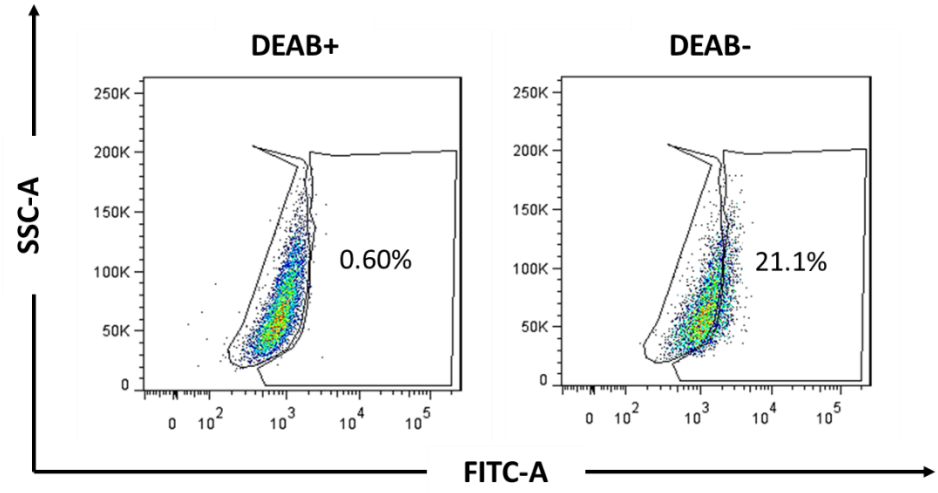

Figure 21. Detection of ALDH activity in the Hs 578T cell line*. Data from one independent experiment.*

Taken together, the obtained results show that the combination of these two markers could possibly be used for the isolation of Hs 578T stem-like cells. However, due to the high percentages of $CD44^{+}$ cells in the cell line (nearly 100%), only the population of cells that are simultaneously $CD44^{high}$ and $ALDH^{+}$ should be selected as being stem-like cells. The expression of CD44 was considered "high" when, by plotting the cells as FSC-H on the Y-axis *versus* APC on the X-axis, the APC-conjugated anti-CD44-stained cells were $>10^{3}$ in the X-axis.

iii. Hs 578T cell line: Isolation of stem-like ($ALDH^{+}/CD44^{high}$) and non-stem ($ALDH^{-}/CD44^{low}$) populations using the BD FACSAria II flow cytometer

Flow cytometric analysis allows the separation and isolation of cells according to different markers.

The isolation of $ALDH^{+}/CD44^{high}$ stem-like cells and $ALDH^{-}/CD44^{low}$ non-stem like cells was performed using the BD FACSAria™ II flow cytometer. Data was analyzed using the BD FACSDiva v8.0.1 software.

In the first assay, three reactions (2 x 10^{5} cells/mL of buffer for each reaction) of ALDEFLUOR™ assay were performed in combination with labelling for CD44 with an allophycocyanin (APC)-conjugated anti-CD44 antibody.

As shown in **Figure 22**, the stem-like cells were sorted by selecting for ALDH$^+$ cells with simultaneous high expression of CD44. The gating for ALDH$^-$ cells with low expression of CD44 was used to sorte the non-stem population. A purity mask was applied to assure that only the defined cells were selected. The cell sorting results obtained using this approach (**Table 7**) showed that the % of putative cancer stem cells isolated was only 0.6% (% total, which means 0.6% of the total number of cells analyzed), which corresponded to ~ 500 events sorted (each event was considered as one single cell). The % of sorted non-stem cells was 5.9%. Since a purity mask was applied, the % of the presumed CSCs was supposed to decrease when compared with the % found above in section ii, however, such low percentages were not expected.

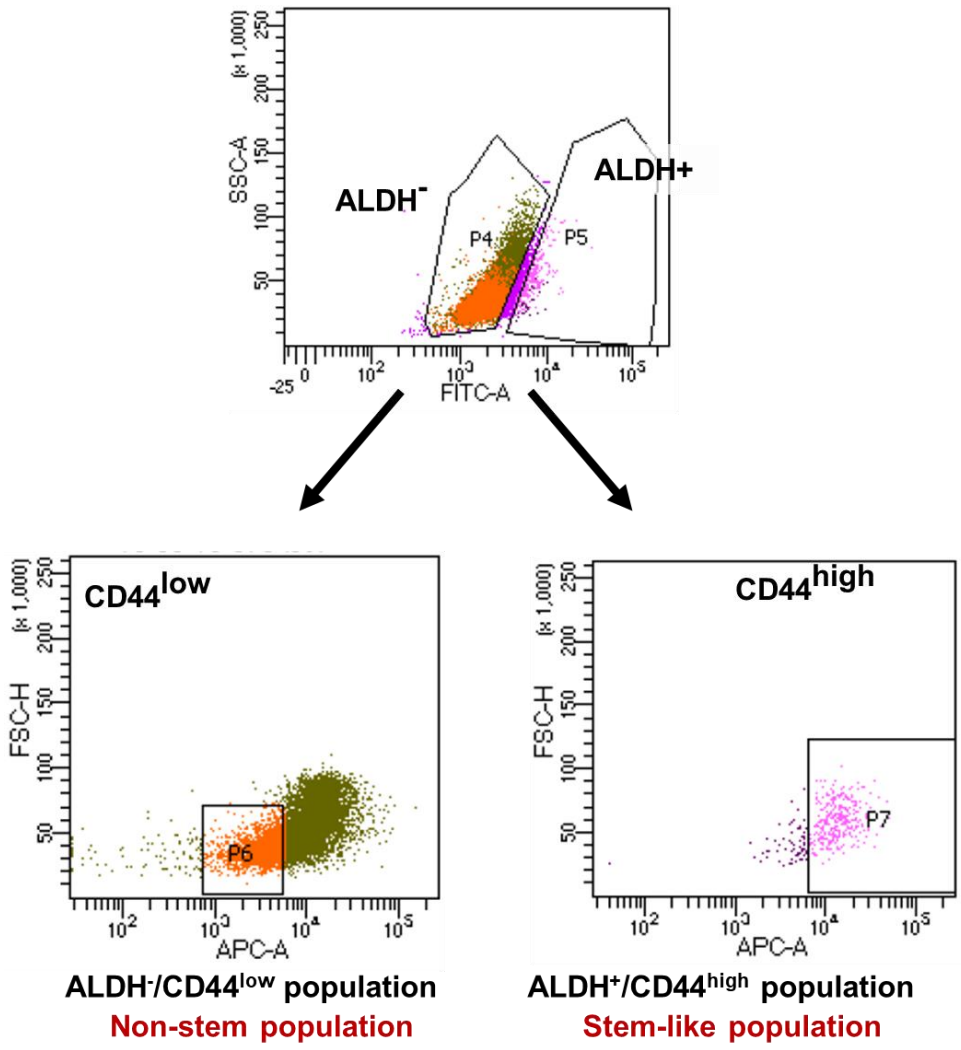

Figure 22. ALDH$^+$/CD44^{high} and ALDH$^-$/CD44^{low} sorted populations. *The ALDEFLUOR™ assay was performed in the Hs 578T cell line in combination with labelling for CD44 with an APC-conjugated anti-CD44 antibody. Single fluorescent markers were used to adjust the photomultiplier tube (PMT) voltages and set up compensations. Data was analyzed using the BD FACSDiva v8.0.1 software. The **P4** population represents the ALDH$^-$ cells and the **P5** population represents de ALDH$^+$ cells. The **P6** and **P8** populations represent the sorted ALDH$^-$/CD44^{low} and ALDH$^+$/CD44^{high} populations respectively. Data from one experiment.*

Table 7. Putative percentages of the sorted populations. *Data from one experiment.*

Population	#Events	%Parent	%Total
P4	10,840	88.3	21.3
P6	3,012	27.8	5.9
P5	380	3.1	0.7
P7	318	83.7	0.6

P4, $ALDH^-$ cells; **P5**, $ALDH^+$ cells; **P6**, $ALDH^-/CD44^{low}$ population; **P7**, $ALDH^+/CD44^{high}$ population. The "% Total" corresponds to the % from the total population of cells used. "%Parent" corresponds to the % from the "parent" group.

Therefore, in order to increase the % of CSCs obtained, in the second assay the number of cells was increased to 3 x 10^6 cells/ mL of buffer. Consequently, three reactions (3 x 10^6 cells/mL of buffer for each reaction) of ALDEFLUOR™ assay were performed in combination with labelling for CD44 with an allophycocyanin (APC)-conjugated anti-CD44 antibody.

By plotting the cells as FSC-H on the Y-axis *versus* APC on the X-axis, the gates for $CD44^{low}$ were defined (**Figure 23**). The expression of CD44 was considered "low" when the APC-conjugated anti-CD44-stained cells were <10^3 in the X-axis. Inversely, the expression of CD44 was considered "high" when the APC-conjugated anti-CD44-stained cells were >10^3 in the X-axis.

.

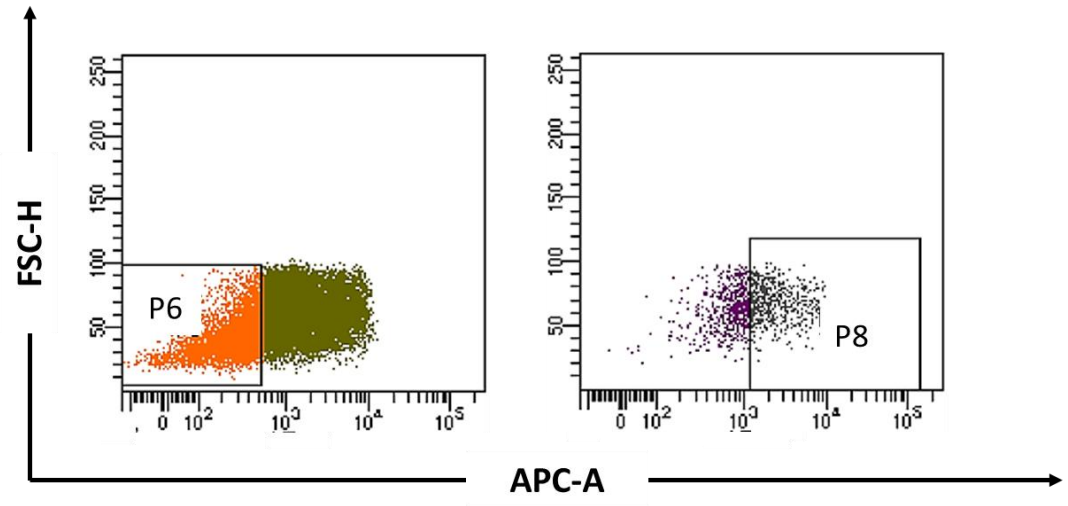

Figure 23. $ALDH^+/CD44^{high}$ and $ALDH^-/CD44^{low}$ sorted populations. *The ALDEFLUOR™ assay was performed in the Hs 578T cell line in combination with labelling for CD44 with an APC-conjugated anti-CD44 antibody. Single fluorescent markers were used to adjust the photomultiplier tube (PMT) voltages and set up compensations. Data was analyzed using the BD FACSDiva v8.0.1 software. The P6 and P8 populations represent the sorted $ALDH^-/CD44^{low}$ and $ALDH^+/CD44^{high}$ populations respectively. Data from one experiment*

The obtained results show (**Table 8**) that the presumed % of ALDH$^+$/CD44^{high} cells was increased to 0.9% (still very low) and the % of isolated cells ALDH$^-$/CD44^{low} was 10.4%.

Table 8. Putative percentages of the sorted populations. *Data from one experiment*

Population	#Events	%Parent	%Total
P4	21,793	83.8	35.4
P6	6,386	29.3	10.4
P5	1,117	4.3	1.8
P8	547	49.0	0.9

P4, ALDH$^-$ cells; **P5**, ALDH$^+$ cells; **P6**, ALDH$^-$/CD44^{low} population; **P8**, ALDH$^+$/CD44^{high} population. The "% Total" corresponds to the % from the total population of cells used. "%Parent" corresponds to the % from the "parent" group.

As the % obtained for isolated ALDH$^+$/CD44^{high} cells was still considerably low, in the third assay these conditions were maintained, but instead of 3 reactions, 4 reactions for ALDEFLUOR^{TM} assay were performed, in order to increase the number of cells analyzed.

The cell sorting results obtained using this approach showed that the % of the putative cancer stem cell population was 1.7% (**Table 9**), which corresponded to ~ 24 168 events sorted. The % of non-stem cells sorted was 8.9%, which corresponded to ~ 259 372 events.

Given these %, the obtained ALDH$^+$/CD44^{high} and ALDH$^-$/CD44^{low} cells were seeded to verify if they recovered /attached.

Table 9. Putative percentages of the sorted populations. *Data from one experiment*

Population	#Events	%Parent	%Total
P4	20,125	81.8	37.5
P6	4,773	23.7	8.9
P5	1,169	4.8	2.2
P8	928	79.4	1.7

P4, ALDH$^-$ cells; **P5**, ALDH$^+$ cells; **P6**, ALDH$^-$/CD44^{low} population; **P8**, ALDH$^+$/CD44^{high} population. The "% Total" corresponds to the % from the total population of cells used. "%Parent" corresponds to the % from the "parent" group.

Maintaining the same conditions but performing 5 reactions for the ALDEFLUOR™ assay in combination with labelling for CD44 with an APC-conjugated anti-CD44 antibody, the results obtained in the fourth assay show a decrease in the % of $ALDH^+/CD44^{high}$ to 0.2% (**Table 10**). Given the previous results obtained, this low % was not expected. This analysis was repeated, and a similar low % of putative CSCs was detected in the three independent assays performed.

Table 10. Putative percentages of the sorted populations. *Representative data from three independent experiments.*

Population	#Events	%Parent	%Total
P4	47,762	95.1	57.0
P6	2,647	5.5	3.2
P5	247	0.5	0.3
P8	181	73.3	0.2

P4, $ALDH^-$ cells; **P5**, $ALDH^+$ cells; **P6**, $ALDH^-/CD44^{low}$ population; **P8**, $ALDH^+/CD44^{high}$ population. The "% Total" corresponds to the % from the total population of cells used. "%Parent" corresponds to the % from the "parent" group.

The use of the ALDEFLUOR™ assay, for the isolation and identification of CSCs, has been increasing. However, in some cases, different published works show different percentages of $ALDH^+$ cells for the same cell line. Regarding the Hs 578T cell line, using the same assay, Stanford *et al.* [122] detected approximately 5 % of cells expressing high levels of ALDH1 activity. However, Mohammadalipour *et al.* [120] detected approximately 20% of ALDH positive cells (which are in concordance with the initial results with had previously obtained in the characterization of the cells (**section ii.**). One possible explanation could be the different densities of the cell culture before the assay. Some authors argue that culture densities can affect the $ALDH^+$ populations, which may express different ALDH isoforms depending on the cells density. In this regard, Lynn *et al.* verified that, in colon cancer, at high cell densities, there is a decrease of $ALDH^+$ cells [123]. To prove this, it would be necessary to characterize the ALDH1 expression in the Hs 578T cell line at different cell densities. It might also be interesting to characterize the presence of these markers using other techniques, such as Western blot analyses.

iv. Analyzing the recovery of the sorted Hs 578T stem-like cells

In order to determine if enough putative CSCs and non-cancer stem cells were obtained to analyze the effects of CUR and CUR-loaded nanoparticles, it was decided to examine the growth of these two populations after cell sorting. With that purpose, the SRB assay was performed and optical densities (OD) were measured. This SRB assay was performed in cells that had been allowed to attach for 24h and in cells that had been allowed to attach for 48h, in order to determine which of these times (24 or 48h) was better to allow cells to attach (before starting experiments).

Therefore, after cell sorting, both the $ALDH^+/CD44^{high}$ and $ALDH^-/CD44^{low}$ cells were plated in 96-well plates (T0 and T96). The T0 plates were analyzed 24 or 48 hours after plating. The SRB assay was initiated at those time points (24 or 48 hours). Cell growth was analyzed (by measuring OD values) 96h after that.

Results from the obtained OD values are presented in **Table 11**.

Table 11.. Cell growth (analyzed as OD values obtained from the SRB assay) from $ALDH^+/CD44^{high}$ and $ALDH^-/CD44^{low}$ sorted cells, following 24h or 48h of cell recovering time. *Data from one independent experiment.*

	OD values			
	24 hours		48 hours	
	TO	T96	TO	T96
$ALDH^+/CD44^{high}$	0,04	0,19	0,06	0,34
$ALDH^-/CD44^{low}$	0,03	0,14	0,05	0,28

The obtained results show that when cells had been allowed to recover for 24 hours, there was an increase in OD (representative of the number of cells) of 4.5x and 5.3x between the T0 and the T96, in the $ALDH^+/CD44^{high}$ and $ALDH^-/CD44^{low}$ populations, respectively. Moreover, when cells had been allowed to recover for 48 hours, there was a higher increase in cell growth, of 6x and 6.3x between the T0 to the T96 in the $ALDH^+/CD44^{high}$ and $ALDH^-/CD44^{low}$ populations, respectively. These results suggest that it is better to allow cells to recover for 48 hours rather than 24 hours.

Due to the obtained low percentage of sorted stem-like cells, the cell number necessary to perform the cytotoxic experiments was not achieved. Therefore, it was not possible to

test, within the time allowed to perform this work, the cytotoxic effect of CUR and CUR NPs in the sorted stem-like populations.

Conclusion

Conclusion and future perspectives

Natural products have gained important attention in the field of drug discovery due to their availability and since they are a source of bioactive compounds, many of them having antitumor potential [86, 124]. Indeed, an important proportion of anti-cancer drugs used in the clinic (such as camptothecin, taxol, epipodophyllotoxin, vinca alkaloids and combrestatin) are derived from plant sources [125]. Nevertheless, there is a continuous need to search new natural agents with low cytotoxic and side-effects, being capable of inhibiting tumor cell proliferation pathways without affecting the non-tumor cells [71]. The first aim of this project was to analyze the antitumor activity of the natural extracts *Melissa Officinalis L.* and *Eucalyptus globulus L.* in the human breast cancer Hs 578T and BT-20 cell lines.

The results here presented showed that the natural extracts have different effects in the two breast cancer cells studied. Both extracts are more potent in the Hs 578T cell line, suggesting that the extracts might have a specific effect in some cells. Even though the cytotoxic effect of both extracts is similar in the two cell lines tested, the extract *Melissa Officinalis L*. is slightly more potent than the *Eucalyptus globulus L* extract, in the Hs 578T cell line.

Several studies have demonstrated that CUR (an isolated compound from the rhizome of Turmeric), by modulating cellular signaling pathways, exerts antitumor effects both *in vitro and in vivo*, which supports the idea that CUR can be considered a promising and potent anticancer agent [126, 127]. However, due to its reduced solubility and low bioavailability, its clinical efficacy is limited. Therefore, several approaches have been attempted to overcome its limitations [82].

Thus, in an attempt to improve CUR bioavailability and solubility, the second aim of this work was to develop curcumin loaded PLGA nanoparticles via a nanoprecipitation technique. To achieve this, three different initial concentrations of CUR were tested (0.1mg, 0.5mg and 1mg). It was verified that the NPs prepared with an initial CUR concentration of 0.5 mg have a smaller particle size, a higher percentage of encapsulation and a homogeneous formulation. These characteristics may improve their cytotoxic effects in cells. Therefore, this formulation was selected for the analysis of the antitumor activity of CUR-loaded PLGA NPs in the Hs 578T cell line. Contrary to other studies [107, 113], the obtained results showed that CUR exhibits more cell growth inhibitory activity than the CUR-loaded NPs. However, it is possible that better results would be obtained under different experimental conditions (e.g. longer treatments or different nanoparticles).

Furthermore, studies were conducted to characterize and isolate breast CSCs from the Hs 578T cell line. CSCs are believed to be responsible for tumor growth and are frequently associated with tumor metastasis, heterogeneity, cancer treatment failure and recurrent lesions. Consequently, CSCs identification is extremely valuable for the development of more effective treatments [38, 40]. Two specific markers were selected for the Hs 578T breast cancer stem cells isolation: ALDH1 enzymatic activity and high expression of the cell surface marker CD44. Flow cytometric analyzes of the proportion of these markers in Hs 578T cells revealed that these cells are highly enriched in $CD44^+$ and also present $ALDH^+$ cells, which suggested that the combination of these markers could be used for the isolation of stem-like cells. After several optimizations of the putative CSCs isolation method, it was possible to isolate some (but very few) $ALDH^+/CD44^{high}$ cells, representative of the stem-like population, and some (a few more) $ALDH^-/CD44^{low}$ cells, representative of the non-stem like cells. However, the attained % of putative CSCs was not enough to perform the cytotoxic experiments with CUR and CUR-loaded nanoparticles.

In conclusion, *Melissa Officinalis L*. and *Eucalyptus Globulus L*. have dose-dependent cytotoxic effects in both the TNBC cell lines tested, being more potent in the Hs 578T cells. The CUR and CUR-loaded nanoparticles also presented dose-dependent cytotoxic effect. However, the CUR-loaded nanoparticles presented lower cytotoxic effect than CUR alone. Thus, further studies should be undertaken to improve the CUR-loaded nanoparticles effect. One possible approach would be to test different stabilizers or different concentrations of the used stabilizer, as previously mentioned.

In addition, preliminary results suggested that is possible to isolate stem-like cells from the Hs 578T cell line, using the specific markers ALDH1 enzymatic activity and high expression of the cell surface marker CD44. Nevertheless, it was not possible to isolate the expected number of putative CSCs to evaluate the cytotoxic effect of the compounds (CUR and CUR-loaded nanoparticles) in the isolated CSCs population. Consequently, new conditions should be optimized for the effective isolation of CSCs, as for example by characterizing the ALDH1 expression in cells at different cell densities. It might also be interesting to characterize the presence of these markers using other techniques, such as Western blot analyses. Moreover, the use of different combinations of stem cell markers should be attempted.

References

[1] L. L. Campbell and K. Polyak, "Breast tumor heterogeneity: cancer stem cells or clonal evolution?," *Cell Cycle,* vol. 6, no. 19, pp. 2332-8, Oct 1 2007.
[2] M. Greaves and C. C. Maley, "Clonal evolution in cancer," *Nature,* vol. 481, no. 7381, pp. 306-13, Jan 18 2012.
[3] M. J. Thun, J. O. DeLancey, M. M. Center, A. Jemal, and E. M. Ward, "The global burden of cancer: priorities for prevention," *Carcinogenesis,* vol. 31, no. 1, pp. 100-10, Jan 2010.
[4] (july 2018). *GLOBOCAN 2012*. Available: http://globocan.iarc.fr/Default.aspx
[5] T. N. Seyfried, R. E. Flores, A. M. Poff, and D. P. D'Agostino, "Cancer as a metabolic disease: implications for novel therapeutics," *Carcinogenesis,* vol. 35, no. 3, pp. 515-27, Mar 2014.
[6] D. Hanahan and R. A. Weinberg, "The hallmarks of cancer," *Cell,* vol. 100, no. 1, pp. 57-70, Jan 7 2000.
[7] P. Pratheeshkumar *et al.*, "Cancer prevention with promising natural products: mechanisms of action and molecular targets," *Anticancer Agents Med Chem,* vol. 12, no. 10, pp. 1159-84, Dec 2012.
[8] M. Schnekenburger, M. Dicato, and M. Diederich, "Plant-derived epigenetic modulators for cancer treatment and prevention," *Biotechnol Adv,* vol. 32, no. 6, pp. 1123-32, Nov 1 2014.
[9] B. Vogelstein and K. W. Kinzler, "Cancer genes and the pathways they control," *Nat Med,* vol. 10, no. 8, pp. 789-99, Aug 2004.
[10] D. Hanahan and R. A. Weinberg, "Hallmarks of cancer: the next generation," *Cell,* vol. 144, no. 5, pp. 646-74, Mar 4 2011.
[11] P. Anand *et al.*, "Cancer is a preventable disease that requires major lifestyle changes," *Pharm Res,* vol. 25, no. 9, pp. 2097-116, Sep 2008.
[12] D. Belpomme *et al.*, "The multitude and diversity of environmental carcinogens," *Environ Res,* vol. 105, no. 3, pp. 414-29, Nov 2007.
[13] S. D. Horne, S. A. Pollick, and H. H. Heng, "Evolutionary mechanism unifies the hallmarks of cancer," *Int J Cancer,* vol. 136, no. 9, pp. 2012-21, May 1 2015.
[14] S. L. Floor, J. E. Dumont, C. Maenhaut, and E. Raspe, "Hallmarks of cancer: of all cancer cells, all the time?," *Trends Mol Med,* vol. 18, no. 9, pp. 509-15, Sep 2012.
[15] Y. A. Fouad and C. Aanei, "Revisiting the hallmarks of cancer," *Am J Cancer Res,* vol. 7, no. 5, pp. 1016-1036, 2017.
[16] P. L. Porter, "Global trends in breast cancer incidence and mortality," *Salud Publica Mex,* vol. 51 Suppl 2, pp. s141-6, 2009.
[17] J. Ferlay *et al.*, "Cancer incidence and mortality worldwide: sources, methods and major patterns in GLOBOCAN 2012," *Int J Cancer,* vol. 136, no. 5, pp. E359-86, Mar 1 2015.
[18] H. B. Nichols *et al.*, "From menarche to menopause: trends among US Women born from 1912 to 1969," *Am J Epidemiol,* vol. 164, no. 10, pp. 1003-11, Nov 15 2006.
[19] E. Altobelli and A. Lattanzi, "Breast cancer in European Union: an update of screening programmes as of March 2014 (review)," *Int J Oncol,* vol. 45, no. 5, pp. 1785-92, Nov 2014.
[20] B. Fleisher, A. N. Brown, and S. Ait-Oudhia, "Application of pharmacometrics and quantitative systems pharmacology to cancer therapy: The example of luminal a breast cancer," *Pharmacol Res,* vol. 124, pp. 20-33, Oct 2017.
[21] H. G. Russnes, O. C. Lingjaerde, A. L. Borresen-Dale, and C. Caldas, "Breast Cancer Molecular Stratification: From Intrinsic Subtypes to Integrative Clusters," *Am J Pathol,* vol. 187, no. 10, pp. 2152-2162, Oct 2017.
[22] K. Subik *et al.*, "The Expression Patterns of ER, PR, HER2, CK5/6, EGFR, Ki-67 and AR by Immunohistochemical Analysis in Breast Cancer Cell Lines," *Breast Cancer (Auckl),* vol. 4, pp. 35-41, May 20 2010.
[23] C. M. Perou *et al.*, "Molecular portraits of human breast tumours," *Nature,* vol. 406, no. 6797, pp. 747-52, Aug 17 2000.
[24] T. Sorlie *et al.*, "Gene expression patterns of breast carcinomas distinguish tumor subclasses with clinical implications," *Proc Natl Acad Sci U S A,* vol. 98, no. 19, pp. 10869-74, Sep 11 2001.

[25] A. Prat and C. M. Perou, "Deconstructing the molecular portraits of breast cancer," *Mol Oncol,* vol. 5, no. 1, pp. 5-23, Feb 2011.
[26] D. L. Holliday and V. Speirs, "Choosing the right cell line for breast cancer research," *Breast Cancer Res,* vol. 13, no. 4, p. 215, Aug 12 2011.
[27] M. Ignatiadis and C. Sotiriou, "Luminal breast cancer: from biology to treatment," *Nat Rev Clin Oncol,* vol. 10, no. 9, pp. 494-506, Sep 2013.
[28] S. Dent, B. Oyan, A. Honig, M. Mano, and S. Howell, "HER2-targeted therapy in breast cancer: a systematic review of neoadjuvant trials," *Cancer Treat Rev,* vol. 39, no. 6, pp. 622-31, Oct 2013.
[29] W. Grubb, R. Young, J. Efird, C. Jindal, and T. Biswas, "Local therapy for triple-negative breast cancer: a comprehensive review," *Future Oncol,* vol. 13, no. 19, pp. 1721-1730, Aug 2017.
[30] V. G. Abramson, B. D. Lehmann, T. J. Ballinger, and J. A. Pietenpol, "Subtyping of triple-negative breast cancer: implications for therapy," *Cancer,* vol. 121, no. 1, pp. 8-16, Jan 1 2015.
[31] B. D. Lehmann *et al.*, "Identification of human triple-negative breast cancer subtypes and preclinical models for selection of targeted therapies," *J Clin Invest,* vol. 121, no. 7, pp. 2750-67, Jul 2011.
[32] B. D. Lehmann, J. A. Pietenpol, and A. R. Tan, "Triple-negative breast cancer: molecular subtypes and new targets for therapy," *Am Soc Clin Oncol Educ Book,* pp. e31-9, 2015.
[33] S. G. Ahn, S. J. Kim, C. Kim, and J. Jeong, "Molecular Classification of Triple-Negative Breast Cancer," *J Breast Cancer,* vol. 19, no. 3, pp. 223-230, Sep 2016.
[34] B. D. Lehmann and J. A. Pietenpol, "Identification and use of biomarkers in treatment strategies for triple-negative breast cancer subtypes," *J Pathol,* vol. 232, no. 2, pp. 142-50, Jan 2014.
[35] P. F. Peddi, M. J. Ellis, and C. Ma, "Molecular basis of triple negative breast cancer and implications for therapy," *Int J Breast Cancer,* vol. 2012, p. 217185, 2012.
[36] A. Prat *et al.*, "Phenotypic and molecular characterization of the claudin-low intrinsic subtype of breast cancer," *Breast Cancer Res,* vol. 12, no. 5, p. R68, 2010.
[37] K. Dias *et al.*, "Claudin-Low Breast Cancer; Clinical & Pathological Characteristics," *PLoS One,* vol. 12, no. 1, p. e0168669, 2017.
[38] S. Q. Geng, A. T. Alexandrou, and J. J. Li, "Breast cancer stem cells: Multiple capacities in tumor metastasis," *Cancer Lett,* vol. 349, no. 1, pp. 1-7, Jul 10 2014.
[39] M. Shackleton, E. Quintana, E. R. Fearon, and S. J. Morrison, "Heterogeneity in cancer: cancer stem cells versus clonal evolution," *Cell,* vol. 138, no. 5, pp. 822-9, Sep 4 2009.
[40] M. F. Clarke *et al.*, "Cancer stem cells--perspectives on current status and future directions: AACR Workshop on cancer stem cells," *Cancer Res,* vol. 66, no. 19, pp. 9339-44, Oct 1 2006.
[41] E. Sugihara and H. Saya, "Complexity of cancer stem cells," *Int J Cancer,* vol. 132, no. 6, pp. 1249-59, Mar 15 2013.
[42] N. A. Lobo, Y. Shimono, D. Qian, and M. F. Clarke, "The biology of cancer stem cells," *Annu Rev Cell Dev Biol,* vol. 23, pp. 675-99, 2007.
[43] B. T. Spike and G. M. Wahl, "p53, Stem Cells, and Reprogramming: Tumor Suppression beyond Guarding the Genome," *Genes Cancer,* vol. 2, no. 4, pp. 404-19, Apr 2011.
[44] H. Mizuno, B. T. Spike, G. M. Wahl, and A. J. Levine, "Inactivation of p53 in breast cancers correlates with stem cell transcriptional signatures," *Proc Natl Acad Sci U S A,* vol. 107, no. 52, pp. 22745-50, Dec 28 2010.
[45] K. E. Hovinga *et al.*, "Inhibition of notch signaling in glioblastoma targets cancer stem cells via an endothelial cell intermediate," *Stem Cells,* vol. 28, no. 6, pp. 1019-29, Jun 2010.
[46] W. Jiang, J. Peng, Y. Zhang, W. C. Cho, and K. Jin, "The implications of cancer stem cells for cancer therapy," *Int J Mol Sci,* vol. 13, no. 12, pp. 16636-57, Dec 5 2012.

[47] P. Grudzien *et al.*, "Inhibition of Notch signaling reduces the stem-like population of breast cancer cells and prevents mammosphere formation," *Anticancer Res,* vol. 30, no. 10, pp. 3853-67, Oct 2010.
[48] N. Takebe *et al.*, "Targeting Notch, Hedgehog, and Wnt pathways in cancer stem cells: clinical update," *Nat Rev Clin Oncol,* vol. 12, no. 8, pp. 445-64, Aug 2015.
[49] M. P. Ablett, J. K. Singh, and R. B. Clarke, "Stem cells in breast tumours: are they ready for the clinic?," *Eur J Cancer,* vol. 48, no. 14, pp. 2104-16, Sep 2012.
[50] P. Ranji, T. Salmani Kesejini, S. Saeedikhoo, and A. M. Alizadeh, "Targeting cancer stem cell-specific markers and/or associated signaling pathways for overcoming cancer drug resistance," *Tumour Biol,* vol. 37, no. 10, pp. 13059-13075, Oct 2016.
[51] C. Ginestier *et al.*, "ALDH1 is a marker of normal and malignant human mammary stem cells and a predictor of poor clinical outcome," *Cell Stem Cell,* vol. 1, no. 5, pp. 555-67, Nov 2007.
[52] A. S. Ribeiro and J. Paredes, "P-Cadherin Linking Breast Cancer Stem Cells and Invasion: A Promising Marker to Identify an "Intermediate/Metastable" EMT State," *Front Oncol,* vol. 4, p. 371, 2014.
[53] T. Chanmee, P. Ontong, K. Kimata, and N. Itano, "Key Roles of Hyaluronan and Its CD44 Receptor in the Stemness and Survival of Cancer Stem Cells," *Front Oncol,* vol. 5, p. 180, 2015.
[54] A. Jaggupilli and E. Elkord, "Significance of CD44 and CD24 as cancer stem cell markers: an enduring ambiguity," *Clin Dev Immunol,* vol. 2012, p. 708036, 2012.
[55] M. Al-Hajj, M. S. Wicha, A. Benito-Hernandez, S. J. Morrison, and M. F. Clarke, "Prospective identification of tumorigenic breast cancer cells," *Proc Natl Acad Sci U S A,* vol. 100, no. 7, pp. 3983-8, Apr 1 2003.
[56] C. Sheridan *et al.*, "CD44+/CD24- breast cancer cells exhibit enhanced invasive properties: an early step necessary for metastasis," *Breast Cancer Res,* vol. 8, no. 5, p. R59, 2006.
[57] S. Ricardo *et al.*, "Breast cancer stem cell markers CD44, CD24 and ALDH1: expression distribution within intrinsic molecular subtype," *J Clin Pathol,* vol. 64, no. 11, pp. 937-46, Nov 2011.
[58] P. Marcato, C. A. Dean, C. A. Giacomantonio, and P. W. Lee, "Aldehyde dehydrogenase: its role as a cancer stem cell marker comes down to the specific isoform," *Cell Cycle,* vol. 10, no. 9, pp. 1378-84, May 1 2011.
[59] S. A. Marchitti, C. Brocker, D. Stagos, and V. Vasiliou, "Non-P450 aldehyde oxidizing enzymes: the aldehyde dehydrogenase superfamily," *Expert Opin Drug Metab Toxicol,* vol. 4, no. 6, pp. 697-720, Jun 2008.
[60] M. Shipitsin *et al.*, "Molecular definition of breast tumor heterogeneity," *Cancer Cell,* vol. 11, no. 3, pp. 259-73, Mar 2007.
[61] A. K. Croker and A. L. Allan, "Inhibition of aldehyde dehydrogenase (ALDH) activity reduces chemotherapy and radiation resistance of stem-like ALDHhiCD44(+) human breast cancer cells," *Breast Cancer Res Treat,* vol. 133, no. 1, pp. 75-87, May 2012.
[62] J. Cui, P. Li, X. Liu, H. Hu, and W. Wei, "Abnormal expression of the Notch and Wnt/beta-catenin signaling pathways in stem-like ALDH(hi)CD44(+) cells correlates highly with Ki-67 expression in breast cancer," *Oncol Lett,* vol. 9, no. 4, pp. 1600-1606, Apr 2015.
[63] K. Chen, Y. H. Huang, and J. L. Chen, "Understanding and targeting cancer stem cells: therapeutic implications and challenges," *Acta Pharmacol Sin,* vol. 34, no. 6, pp. 732-40, Jun 2013.
[64] E. Marangoni *et al.*, "CD44 targeting reduces tumour growth and prevents post-chemotherapy relapse of human breast cancers xenografts," *Br J Cancer,* vol. 100, no. 6, pp. 918-22, Mar 24 2009.
[65] L. Cheng *et al.*, "The clinical and therapeutic implications of cancer stem cell biology," *Expert Rev Anticancer Ther,* vol. 11, no. 7, pp. 1131-43, Jul 2011.
[66] T. Wang *et al.*, "Cancer stem cell targeted therapy: progress amid controversies," *Oncotarget,* vol. 6, no. 42, pp. 44191-206, Dec 29 2015.

[67] T. Feng, Y. Wei, R. J. Lee, and L. Zhao, "Liposomal curcumin and its application in cancer," *Int J Nanomedicine,* vol. 12, pp. 6027-6044, 2017.
[68] U. Banik, S. Parasuraman, A. K. Adhikary, and N. H. Othman, "Curcumin: the spicy modulator of breast carcinogenesis," *J Exp Clin Cancer Res,* vol. 36, no. 1, p. 98, Jul 19 2017.
[69] M. Bhagat, V. Sharma, and A. K. Saxena, "Anti-proliferative effect of leaf extracts of Eucalyptus citriodora against human cancer cells in vitro and in vivo," *Indian J Biochem Biophys,* vol. 49, no. 6, pp. 451-7, Dec 2012.
[70] E. Rajesh, L. S. Sankari, L. Malathi, and J. R. Krupaa, "Naturally occurring products in cancer therapy," *J Pharm Bioallied Sci,* vol. 7, no. Suppl 1, pp. S181-3, Apr 2015.
[71] Q. Liu, W. T. Loo, S. C. Sze, and Y. Tong, "Curcumin inhibits cell proliferation of MDA-MB-231 and BT-483 breast cancer cells mediated by down-regulation of NFkappaB, cyclinD and MMP-1 transcription," *Phytomedicine,* vol. 16, no. 10, pp. 916-22, Oct 2009.
[72] C. da Silva Mde *et al.*, "Nitrogen-fixing bacteria in Eucalyptus globulus plantations," *PLoS One,* vol. 9, no. 10, p. e111313, 2014.
[73] Q. V. Vuong, A. C. Chalmers, D. Jyoti Bhuyan, M. C. Bowyer, and C. J. Scarlett, "Botanical, Phytochemical, and Anticancer Properties of the Eucalyptus Species," *Chem Biodivers,* vol. 12, no. 6, pp. 907-24, Jun 2015.
[74] H. M. Ashour, "Antibacterial, antifungal, and anticancer activities of volatile oils and extracts from stems, leaves, and flowers of Eucalyptus sideroxylon and Eucalyptus torquata," *Cancer Biol Ther,* vol. 7, no. 3, pp. 399-403, Mar 2008.
[75] P. M. Doll-Boscardin *et al.*, "In Vitro Cytotoxic Potential of Essential Oils of Eucalyptus benthamii and Its Related Terpenes on Tumor Cell Lines," *Evid Based Complement Alternat Med,* vol. 2012, p. 342652, 2012.
[76] A. C. de Sousa, D. S. Alviano, A. F. Blank, P. B. Alves, C. S. Alviano, and C. R. Gattass, "Melissa officinalis L. essential oil: antitumoral and antioxidant activities," *J Pharm Pharmacol,* vol. 56, no. 5, pp. 677-81, May 2004.
[77] A. Jahanban-Esfahlan, S. Modaeinama, M. Abasi, M. M. Abbasi, and R. Jahanban-Esfahlan, "Anti Proliferative Properties of Melissa officinalis in Different Human Cancer Cells," *Asian Pac J Cancer Prev,* vol. 16, no. 14, pp. 5703-7, 2015.
[78] D. B. Magalhaes *et al.*, "Melissa officinalis L. ethanolic extract inhibits the growth of a lung cancer cell line by interfering with the cell cycle and inducing apoptosis," *Food Funct,* vol. 9, no. 6, pp. 3134-3142, Jun 20 2018.
[79] M. Carocho *et al.*, "Melissa officinalis L. decoctions as functional beverages: a bioactive approach and chemical characterization," *Food Funct,* vol. 6, no. 7, pp. 2240-8, Jul 2015.
[80] M. A. Encalada *et al.*, "Anti-proliferative effect of Melissa officinalis on human colon cancer cell line," *Plant Foods Hum Nutr,* vol. 66, no. 4, pp. 328-34, Nov 2011.
[81] P. Anand, A. B. Kunnumakkara, R. A. Newman, and B. B. Aggarwal, "Bioavailability of curcumin: problems and promises," *Mol Pharm,* vol. 4, no. 6, pp. 807-18, Nov-Dec 2007.
[82] J. G. Devassy, I. D. Nwachukwu, and P. J. Jones, "Curcumin and cancer: barriers to obtaining a health claim," *Nutr Rev,* vol. 73, no. 3, pp. 155-65, Mar 2015.
[83] A. Kunwar, A. Barik, B. Mishra, K. Rathinasamy, R. Pandey, and K. I. Priyadarsini, "Quantitative cellular uptake, localization and cytotoxicity of curcumin in normal and tumor cells," *Biochim Biophys Acta,* vol. 1780, no. 4, pp. 673-9, Apr 2008.
[84] M. Jiang *et al.*, "Curcumin induces cell death and restores tamoxifen sensitivity in the antiestrogen-resistant breast cancer cell lines MCF-7/LCC2 and MCF-7/LCC9," *Molecules,* vol. 18, no. 1, pp. 701-20, Jan 8 2013.
[85] Y. Li and T. Zhang, "Targeting cancer stem cells by curcumin and clinical applications," *Cancer Lett,* vol. 346, no. 2, pp. 197-205, May 1 2014.
[86] D. Subramaniam *et al.*, "Curcumin induces cell death in esophageal cancer cells through modulating Notch signaling," *PLoS One,* vol. 7, no. 2, p. e30590, 2012.

[87] M. Gaumet, A. Vargas, R. Gurny, and F. Delie, "Nanoparticles for drug delivery: the need for precision in reporting particle size parameters," *Eur J Pharm Biopharm,* vol. 69, no. 1, pp. 1-9, May 2008.
[88] M. M. Yallapu, P. K. Nagesh, M. Jaggi, and S. C. Chauhan, "Therapeutic Applications of Curcumin Nanoformulations," *AAPS J,* vol. 17, no. 6, pp. 1341-56, Nov 2015.
[89] F. Sadat Tabatabaei Mirakabad *et al.*, "PLGA-based nanoparticles as cancer drug delivery systems," *Asian Pac J Cancer Prev,* vol. 15, no. 2, pp. 517-35, 2014.
[90] H. K. Makadia and S. J. Siegel, "Poly Lactic-co-Glycolic Acid (PLGA) as Biodegradable Controlled Drug Delivery Carrier," *Polymers (Basel),* vol. 3, no. 3, pp. 1377-1397, Sep 1 2011.
[91] R. Dinarvand, N. Sepehri, S. Manoochehri, H. Rouhani, and F. Atyabi, "Polylactide-co-glycolide nanoparticles for controlled delivery of anticancer agents," *Int J Nanomedicine,* vol. 6, pp. 877-95, 2011.
[92] J. K. Vasir and V. Labhasetwar, "Biodegradable nanoparticles for cytosolic delivery of therapeutics," *Adv Drug Deliv Rev,* vol. 59, no. 8, pp. 718-28, Aug 10 2007.
[93] F. Danhier, E. Ansorena, J. M. Silva, R. Coco, A. Le Breton, and V. Preat, "PLGA-based nanoparticles: an overview of biomedical applications," *J Control Release,* vol. 161, no. 2, pp. 505-22, Jul 20 2012.
[94] M. M. Yallapu, M. Jaggi, and S. C. Chauhan, "Curcumin nanoformulations: a future nanomedicine for cancer," *Drug Discov Today,* vol. 17, no. 1-2, pp. 71-80, Jan 2012.
[95] V. Vichai and K. Kirtikara, "Sulforhodamine B colorimetric assay for cytotoxicity screening," *Nat Protoc,* vol. 1, no. 3, pp. 1112-6, 2006.
[96] *AldefluorTM Kit*. Available: https://cdn.stemcell.com/media/files/pis/29888-PIS_1_1_2.pdf
[97] W. Voigt, "Sulforhodamine B assay and chemosensitivity," *Methods Mol Med,* vol. 110, pp. 39-48, 2005.
[98] E. A. Orellana and A. L. Kasinski, "Sulforhodamine B (SRB) Assay in Cell Culture to Investigate Cell Proliferation," *Bio Protoc,* vol. 6, no. 21, Nov 5 2016.
[99] P. Skehan *et al.*, "New colorimetric cytotoxicity assay for anticancer-drug screening," *J Natl Cancer Inst,* vol. 82, no. 13, pp. 1107-12, Jul 4 1990.
[100] Y. L. Franco, T. R. Vaidya, and S. Ait-Oudhia, "Anticancer and cardio-protective effects of liposomal doxorubicin in the treatment of breast cancer," *Breast Cancer (Dove Med Press),* vol. 10, pp. 131-141, 2018.
[101] O. A. Bamodu *et al.*, "Ovatodiolide sensitizes aggressive breast cancer cells to doxorubicin, eliminates their cancer stem cell-like phenotype, and reduces doxorubicin-associated toxicity," *Cancer Lett,* vol. 364, no. 2, pp. 125-34, Aug 10 2015.
[102] B. Corkery, J. Crown, M. Clynes, and N. O'Donovan, "Epidermal growth factor receptor as a potential therapeutic target in triple-negative breast cancer," *Ann Oncol,* vol. 20, no. 5, pp. 862-7, May 2009.
[103] I. Mota, Rodrigues Pinto, P. C., Novo, C., Sousa, G., Guerreiro, O., Guerr,Â. R., "Extraction of Polyphenolic Compounds from Eucalyptus globulus Bark: Process Optimization and Screening for Biological Activity," *Industrial & Engeneering Chemistry Research* 2012.
[104] S. U. Saraydin *et al.*, "Antitumoral effects of Melissa officinalis on breast cancer in vitro and in vivo," *Asian Pac J Cancer Prev,* vol. 13, no. 6, pp. 2765-70, 2012.
[105] T. Choudhuri, S. Pal, M. L. Agwarwal, T. Das, and G. Sa, "Curcumin induces apoptosis in human breast cancer cells through p53-dependent Bax induction," *FEBS Lett,* vol. 512, no. 1-3, pp. 334-40, Feb 13 2002.
[106] M. Kakarala *et al.*, "Targeting breast stem cells with the cancer preventive compounds curcumin and piperine," *Breast Cancer Res Treat,* vol. 122, no. 3, pp. 777-85, Aug 2010.
[107] M. M. Yallapu, B. K. Gupta, M. Jaggi, and S. C. Chauhan, "Fabrication of curcumin encapsulated PLGA nanoparticles for improved therapeutic effects in metastatic cancer cells," *J Colloid Interface Sci,* vol. 351, no. 1, pp. 19-29, Nov 1 2010.

[108] T. T. Tran, P. H. Tran, K. T. Nguyen, and V. T. Tran, "Nano-Precipitation: Preparation and Application in the Field of Pharmacy," *Curr Pharm Des,* vol. 22, no. 20, pp. 2997-3006, 2016.
[109] J. M. Barichello, M. Morishita, K. Takayama, and T. Nagai, "Encapsulation of hydrophilic and lipophilic drugs in PLGA nanoparticles by the nanoprecipitation method," *Drug Dev Ind Pharm,* vol. 25, no. 4, pp. 471-6, Apr 1999.
[110] S. Bhattacharjee, "DLS and zeta potential - What they are and what they are not?," *J Control Release,* vol. 235, pp. 337-351, Aug 10 2016.
[111] T. dos Santos, J. Varela, I. Lynch, A. Salvati, and K. A. Dawson, "Quantitative assessment of the comparative nanoparticle-uptake efficiency of a range of cell lines," *Small,* vol. 7, no. 23, pp. 3341-9, Dec 2 2011.
[112] G. Mittal, D. K. Sahana, V. Bhardwaj, and M. N. Ravi Kumar, "Estradiol loaded PLGA nanoparticles for oral administration: effect of polymer molecular weight and copolymer composition on release behavior in vitro and in vivo," *J Control Release,* vol. 119, no. 1, pp. 77-85, May 14 2007.
[113] P. Anand *et al.*, "Design of curcumin-loaded PLGA nanoparticles formulation with enhanced cellular uptake, and increased bioactivity in vitro and superior bioavailability in vivo," *Biochem Pharmacol,* vol. 79, no. 3, pp. 330-8, Feb 1 2010.
[114] T. Musumeci *et al.*, "PLA/PLGA nanoparticles for sustained release of docetaxel," *Int J Pharm,* vol. 325, no. 1-2, pp. 172-9, Nov 15 2006.
[115] C. R. C. Pietra Renata Celi Carvalho de Souza, Melo Carla Nunes, Rodrigues Lívia Bomfim, Santos Patrícia Campi, Bretz Gabriel Pissolati Matos et al . "Evaluation of polymeric PLGA nanoparticles conjugated to curcumin for use in aPDT," *Braz. J. Pharm. Sci,* 2017.
[116] W. Punfa *et al.*, "Curcumin-loaded PLGA nanoparticles conjugated with anti- P-glycoprotein antibody to overcome multidrug resistance," *Asian Pac J Cancer Prev,* vol. 15, no. 21, pp. 9249-58, 2014.
[117] J. E. Visvader, "Cells of origin in cancer," *Nature,* vol. 469, no. 7330, pp. 314-22, Jan 20 2011.
[118] D. Wu *et al.*, "Aldehyde dehydrogenase 3A1 is robustly upregulated in gastric cancer stem-like cells and associated with tumorigenesis," *Int J Oncol,* vol. 49, no. 2, pp. 611-22, Aug 2016.
[119] Z. Shang *et al.*, "Isolation of cancer progenitor cells from cancer stem cells in gastric cancer," *Mol Med Rep,* vol. 15, no. 6, pp. 3637-3643, Jun 2017.
[120] A. Mohammadalipour, M. M. Burdick, and D. F. J. Tees, "Deformability of breast cancer cells in correlation with surface markers and cell rolling," *FASEB J,* vol. 32, no. 4, pp. 1806-1817, Apr 2018.
[121] M. M. Burdick *et al.*, "Expression of E-selectin ligands on circulating tumor cells: cross-regulation with cancer stem cell regulatory pathways?," *Front Oncol,* vol. 2, p. 103, 2012.
[122] E. A. Stanford *et al.*, "The role of the aryl hydrocarbon receptor in the development of cells with the molecular and functional characteristics of cancer stem-like cells," *BMC Biol,* vol. 14, p. 20, Mar 16 2016.
[123] L. M. Opdenaker, S. R. Modarai, and B. M. Boman, "The Proportion of ALDEFLUOR-Positive Cancer Stem Cells Changes with Cell Culture Density Due to the Expression of Different ALDH Isoforms," *Cancer Stud Mol Med,* vol. 2, no. 2, pp. 87-95, 2015.
[124] A. R. Amin, O. Kucuk, F. R. Khuri, and D. M. Shin, "Perspectives for cancer prevention with natural compounds," *J Clin Oncol,* vol. 27, no. 16, pp. 2712-25, Jun 1 2009.
[125] L. Ouyang *et al.*, "Plant natural products: from traditional compounds to new emerging drugs in cancer therapy," *Cell Prolif,* vol. 47, no. 6, pp. 506-15, Dec 2014.
[126] G. M. Calaf, R. Ponce-Cusi, and F. Carrion, "Curcumin and paclitaxel induce cell death in breast cancer cell lines," *Oncol Rep,* vol. 40, no. 4, pp. 2381-2388, Oct 2018.
[127] S. Hu, Y. Xu, L. Meng, L. Huang, and H. Sun, "Curcumin inhibits proliferation and promotes apoptosis of breast cancer cells," *Exp Ther Med,* vol. 16, no. 2, pp. 1266-1272, Aug 2018.